

Chaos in the Solar System

Myron Lecar, Fred A Franklin, Matthew J Holman

Harvard-Smithsonian Center for Astrophysics, 60 Garden Street, Cambridge, Massachusetts
02138; e-mail: mlecar@cfa.harvard.edu

Norman W Murray

Canadian Institute for Theoretical Astrophysics, McLennan Physical Labs, University of
Toronto, 60 St. George Street, Toronto, Ontario M5S 1A7, Canada; e-mail:
murray@cita.utoronto.ca

KEYWORDS: celestial mechanics, planetary dynamics, Kirkwood gaps

ABSTRACT:

The physical basis of chaos in the solar system is now better understood: in all cases investigated so far, chaotic orbits result from overlapping resonances. Perhaps the clearest examples are found in the asteroid belt. Overlapping resonances account for its Kirkwood gaps and were used to predict and find evidence for very narrow gaps in the outer belt. Further afield, about one new “short-period” comet is discovered each year. They are believed to come from the “Kuiper Belt” (at 40 AU or more) via chaotic orbits produced by mean-motion and secular resonances with Neptune. Finally, the planetary system itself is not immune from chaos. In the inner solar system, overlapping secular resonances have been identified as the possible source of chaos. For example, Mercury, in 10^{12} years, may suffer a close encounter with Venus or plunge into the Sun. In the outer solar system, three-body resonances have been identified as a source of chaos, but

on an even longer time scale of 10^9 times the age of the solar system. On the human time scale, the planets do follow their orbits in a stately procession, and we can predict their trajectories for hundreds of thousands of years. That is because the mavericks, with shorter instability times, have long since been ejected. The solar system is not stable; it is just old!

CONTENTS

INTRODUCTION	2
CHAOS AND CELESTIAL MECHANICS	6
<i>The Origin of Chaos: Overlapping "Mean-Motion" Resonances</i>	10
DYNAMICS IN THE ASTEROID BELT	12
<i>Chaos in the Outer Belt</i>	19
<i>Behavior at First-Order Mean-Motion Resonances</i>	22
LONG-TERM STABILITY OF SMALL BODIES IN THE OUTER SOLAR SYS-	
TEM	28
<i>The Region between Jupiter and Saturn</i>	30
<i>The Regions Between the Other Outer Planets</i>	32
<i>The Inner Solar System</i>	35
<i>The Kuiper Belt</i>	36
PLANETARY CHAOS	41
<i>Numerical Integrations</i>	41
<i>Analytic Results</i>	49
SUMMARY AND SUGGESTIONS FOR FURTHER WORK	55

1 INTRODUCTION

All known cases of chaos in the solar system are caused by overlapping resonances. Brian Marsden and I (ML), when we were students at Yale, had frequent discus-

sions with Dirk Brouwer about the significance of two resonances that overlapped. The “small divisors” that occur in perturbation theory at single resonances can be removed by a change of variables introduced by Poincaré, which results in a resonance Hamiltonian similar to that of a pendulum. No such device was ever discovered for two overlapping resonances, and Brouwer sensed that there was something special about that case. Because a single trajectory can be numerically integrated through an overlapping resonance without apparent catastrophe, I argued forcefully (and incorrectly) that the difficulty with overlapping resonances might just be a defect in the perturbation theory. However, had we numerically integrated a clone, initially differing infinitesimally from the original trajectory, the two would have separated exponentially. In fact, that is the definition of a chaotic orbit: exponential dependence on initial conditions.

In many cases we can estimate the Lyapunov Time (the e-folding time in the above example) and even the Crossing Time (the time for a small body to develop enough eccentricity to cross the orbit of the perturber). Both times depend on the Stochasticity Parameter, which measures the extent of the resonance overlap.

There is evidence that, today, small bodies in the solar system (e.g. comets and asteroids) behave chaotically. Meteorites are thought to be fragments of asteroid collisions. The asteroid Vesta has a reflection spectrum that resembles that of many meteorites. Every so often a meteorite hits the Earth, so we have evidence, within the last hundred years, of chaotic behavior. We have also found meteorites that originated on Mars. We believe they came from Mars because trapped bubbles of gas coincide with samples of the Martian atmosphere.

Kirkwood (1867) noticed that the asteroid belt has “gaps” at resonances, i.e. at distances where the asteroidal periods are a rational fraction of Jupiter’s period.

There have been many attempts to explain these gaps on the basis of a single resonance, but these attempts never produced gaps as devoid of bodies as the observed ones. We now understand that bodies are removed from regions where the overlap of two or more resonances induces chaos and large excursions in the eccentricity. Wisdom (1982, 1983, 1985) first illustrated how chaos at the 3:1 resonance with Jupiter could result in sufficiently large eccentricity to allow an encounter with Mars or the Earth. Subsequent work showed that even collisions with Sun are a likely outcome (Ferraz-Mello & Klafke 1991, Farinella et al 1994). Chaotic dynamics in the asteroid belt will be reviewed in Section 3.

One to two “short period” comets (short means periods less than 200 years) are discovered per year. Short period comets are confined to the ecliptic and are believed to come from the Kuiper Belt, which is located about 40 AU from the Sun, in neighborhood of Pluto. Their stability is also discussed in this review.

In contrast, long period comets are thought to come from the Oort Cloud at 20,000 AU. They are perturbed into the inner solar system by stellar encounters or by the tidal field of the galaxy. These mechanisms differ from those determining the dynamics of short period comets and are not reviewed here.

By now, the entire solar system exterior to Jupiter has been surveyed for stability. Holman & Wisdom (1993) found that all the unpopulated regions of the solar system are unstable, on time scales that, in general, are much less than the age of the solar system. However, some comet orbits in the Kuiper Belt are just now becoming perturbed into the inner solar system. The chaotic dynamics of comets in the outer solar system is reviewed in Section 4.

It is not too alarming that small bodies behave chaotically. Comets and asteroids have individual masses less than 1/1000 that of the Earth and, in total,

make up much less than an Earth's mass. However, we depend on the regularity of the planetary orbits. Could they be chaotic? The answer for the known planets is yes—but on a long time scale. The planets have presumably followed their present orbits for much of the lifetime of the solar system. But for how much longer? Are we in danger of losing a planet soon? Computers are just now able to integrate the planets for the life time of the solar system so we now have a preliminary exploration of this important problem. Here too chaos is induced at resonances, but evidence suggest that they are secular resonances that operate on long time scales.

Earlier, the stability of the solar system was studied by looking for terms in the semimajor axis that grew with the time, (secular terms), or as the time multiplied by a periodic function of the time, (mixed secular terms). Now we know that instability comes from a chaotic growth of the eccentricity. The stability of the planets is reviewed in Section 4.

For the reader who is intrigued, but new to this subject, we suggest a popular book called *Newton's Clock: Chaos in the Solar System* by mathematician Ivars Peterson (1993). We refer all readers to the earlier review by Duncan & Quinn entitled "The Long-Term Dynamical Evolution of the Solar System," which appeared in the 1993 edition of this Annual Review. In addition, the proceedings of the 1996 workshop on "Chaos in Gravitational N-Body Systems" have appeared as a book and in Volume 64 of *Celestial Mechanics and Dynamical Astronomy*.

Hénon (1983) gives a lucid introduction to chaotic orbits and the "surface of section" technique. Ott (1993) has written the standard text on chaos which covers a variety of physical problems. Sagdeev et al (1988) review other interesting applications of chaos including turbulence.

2 CHAOS AND CELESTIAL MECHANICS

The rigorous condition for a mechanical system to be stable for all time is that there exists an “integral” (a conserved quantity) for each degree of freedom. The Sun and one planet is just such a system (e.g. the Kepler Problem). Fortunately, because the Sun is 1000 times more massive than Jupiter and the rest of the planets add up to less than a Jupiter mass, treating the planets as independent two-body problems is an excellent starting approximation. Using their “Keplerian” orbits, one can calculate a first approximation to their forces on each other. Successive iterations of that procedure, carried out with great sophistication, are the techniques called celestial mechanics. The classic text on celestial mechanics was written by Brouwer & Clemence (1961). See *Solar System Dynamics* by Murray & Dermott (1999) for a recent treatment.

Much of the history of celestial mechanics has involved the search for integrals of motion. The search was doomed to fail; eventually Poincaré proved that there was no analytic integral for the problem of the Sun and two planets. However, there do exist nonanalytic integrals. Their discovery culminated in the Kolmogorov-Arnold-Moser (KAM) theorem, a fundamental result in the mathematics of chaos. The theorem guarantees the existence of “invariant curves” (i.e. other integrals) as long as the perturbations are not too large and the coupling is not too near any resonance. Understanding the exact meaning of the word *near* was crucial, because resonances (like the rational numbers) are dense. This theorem is discussed in *The Transition to Chaos* by Reichl (1992) and in *Regular and Chaotic Dynamics* by Lichtenberg & Leiberman (1992) (our recommended text). For the more mathematically minded, there is also a set of lectures by Moser called *Stable and Random Motions in Dynamical Systems* (1973) and

Mathematical Methods of Classical Mechanics by Arnold (1978).

Although the KAM theorem is of fundamental importance for the mathematical structure of chaos, the strict conditions of the theorem are satisfied in the solar system. In what follows, we will be concerned with orbits that are not covered by the KAM theorem.

All of the analytic work described in this review relies on perturbation theory, exploiting the fact that the planetary masses are small compared with the mass of the Sun. A brief outline of the approach follows.

The equation of motion of a planet orbiting a star accompanied by a second planet is

$$\frac{d^2 \mathbf{r}_1}{dt^2} + \mathcal{G}(M_\odot + M_1) \frac{\mathbf{r}_1}{r_1^3} = \nabla_1 R_{1,2}, \quad (1)$$

where

$$R_{1,2} = \mathcal{G}M_2 \left[\frac{1}{r_{1,2}} - \frac{\mathbf{r}_1 \cdot \mathbf{r}_2}{r_2^3} \right] \quad (2)$$

Here r_1 is the distance between the Sun and planet 1, and $r_{1,2} \equiv \sqrt{(\mathbf{r}_1 - \mathbf{r}_2)^2}$ is the distance between the planets. The quantity R , which is the negative of the planetary potential, is known as the disturbing function; it describes the disturbances of the planet's elliptical orbit produced by the other planet. The second term in the square brackets arises from the noninertial nature of the coordinate system employed and is known as the "indirect" term. It occurs because the traditional coordinate system takes the position of the sun as the origin. It is not generally relevant to the chaotic behavior of bodies in the solar system, so we ignore it henceforth.

The next step is to expand the disturbing function using the expressions for r_i and θ_i found by solving the Kepler problem. This rather daunting task has been performed by a number of authors (Peirce 1849, Le Verrier 1855, Murray &

Harper 1993). The general form is

$$R_{1,2} = \frac{\mathcal{G}M_2}{a_2} \sum_{\mathbf{j}} \phi_{\mathbf{j}}(a_1, a_2) e_1^{|j_3|} e_2^{|j_4|} i_1^{|j_5|} i_2^{|j_6|} \times \cos [j_1 \lambda_1 + j_2 \lambda_2 + j_3 \varpi_1 + j_4 \varpi_2 + j_5 \Omega_1 + j_6 \Omega_2]. \quad (3)$$

In this expression the j_i are positive and negative integers. The angles in the argument of the cosine are the mean, apsidal, and nodal longitudes and are measured from the x-axis. If we rotate the coordinate system, the disturbing function, which is proportional to a physical quantity (the force), cannot change. This implies that $\sum_i j_i = 0$. We have kept only the lowest order terms in the sum; for a given $|j_i|$ terms proportional to $e^{|j_i|+1}$ or larger powers will also appear. Each cosine represents a resonance; the effects of these resonances constitute the subject of this review.

We can use this expression to find the effect of one planet on another. Hamilton's formulation of mechanics offers the easiest way to proceed. Using action-angle variables for the two body problem, the quantities λ , $-\varpi$, and $-\Omega$ are appropriate angles. The corresponding actions are simple functions of a , e , and i : $L \equiv \sqrt{\mathcal{G}Ma}$, $G \equiv \sqrt{\mathcal{G}Ma}[1 - \sqrt{(1 - e^2)}] \approx (1/2)e^2 L$, and $H \equiv \sqrt{\mathcal{G}Ma(1 - e^2)}(1 - \cos i) \approx (1/2)i^2 L$, where we have distinguished the gravitational constant, \mathcal{G} , from the momentum, G . In these variables the Kepler Hamiltonian is $\mathcal{H} = (\mathcal{G}M)/2L^2$. Because we are using action-angle variables, none of the angles appear. This tells us immediately that the motion takes place on three-dimensional surfaces in phase space, defined by L , G and H held constant. Topologically, this is a three-torus. The surprising thing is that G and H do not appear in the Hamiltonian, so that ϖ and Ω are also constant. In a generic three degree of freedom Hamiltonian one would expect all three actions to appear explicitly, leading to three non-constant angles. The Kepler problem is degenerate, as is reflected in

the fact that H and G do not appear in \mathcal{H} . In this case the motion takes place on a one-torus, or circle, in phase space.

To find the variation in a , for example, note that

$$\frac{dL_1}{dt} = \frac{1}{2} \frac{L_1}{a_1} \frac{da_1}{dt}, \quad (4)$$

so

$$\frac{da_1}{dt} = 2 \frac{a_1}{L_1} \frac{\partial R}{\partial \lambda_1}. \quad (5)$$

The presence of planet 2 forces periodic variations in the semimajor axis of planet

1. For example, suppose we pick a term of the form

$$\phi_{2,-5,3,0,0,0}(a_1, a_2) e_1^3 \cos[2\lambda_1 - 5\lambda_2 + 3\varpi_1]. \quad (6)$$

The equation for a_1 becomes

$$\frac{da_1}{dt} = -4(a_1 n_1) \frac{a_1 M_2}{a_2 M} \phi_{2,-5,3,0,0,0}(a_1, a_2) e_1^3 \sin[2\lambda_1 - 5\lambda_2 + 3\varpi_1] + O(e)^4. \quad (7)$$

Similar expressions can be derived for all the other orbital elements.

With these expressions, or similar ones provided by Lagrange, it appeared to be a simple matter to integrate the equations of motion. However, early efforts to do so revealed difficulties. The problem can be seen by integrating equation (7). To first order in M_2 we find

$$a_1(t) - a_1(0) = a_1 \frac{a_1 M_2}{a_2 M} \frac{n_1}{2n_1 - 5n_2 + 3\dot{\varpi}_1} \phi_{2,-5,3,0,0,0}(a_1, a_2) e_1^3 \cos[2\lambda_1 - 5\lambda_2 + 3\varpi_1] + O(e)^4. \quad (8)$$

The denominator $2n_1 - 5n_2 + 3\dot{\varpi}_1$, and similar denominators that arise when all the terms in the disturbing function are considered, is the source of the difficulty. Poincaré (1993) pointed out that for integers j_1 and j_2 (2 and 5 in our example) the denominator becomes arbitrarily small. He went on to show that, in spite

of the fact that terms with large j_1 and j_2 tend to carry large powers of the eccentricities, the sums used to define the hoped-for analytic solutions diverged.

The locations in phase space (essentially along the a axis) where the denominator vanishes are known as resonances. Poincaré noted that in the immediate vicinity of a resonance the motion was very complicated. Later work, particularly that of Chirikov (1979), showed that the complicated motion, dubbed chaos, occupied a large fraction of the phase space near the resonance when two neighboring resonances overlapped. This result is essentially an anti-KAM theorem, in that it specifies where KAM tori are absent. It provides the underpinnings of much of the work reviewed in this article.

2.1 The Origin of Chaos: Overlapping “Mean-Motion” Resonances

The chaos generated at overlapping resonances was first studied, in the astronomical context, by Wisdom (1980), who calculated the width and extent of overlap of adjacent first-order resonances in the circular restricted three-body problem and found that they overlap to a distance given by $\delta a/a \sim 1.3\mu^{2/7}$, where μ is the mass ratio of the planet to the central star. The resonance overlap criterion for chaos was developed by Chirikov (1979). The width of the first-order resonances, for zero eccentricity, in the restricted problem was also derived by Franklin et al (1984), from which we find that the 2:1 mean-motion resonance extends, in semimajor axis (with $a_{Jupiter} = 1$) from 0.621 to 0.639, the 3:2 from 0.749 to 0.778, the 4:3 from 0.808 to 0.843, the 5:4 from 0.841 to 0.883, and the 6:5 from 0.863 to 0.908. The 4:3 overlaps with the 5:4 and all adjacent resonances closer to Jupiter overlap. The 4:3 resonance is at 0.825; the Wisdom formula predicts onset of chaos for $a > 0.82$. This region where mean-motion resonances overlap

is where the relation between the Lyapunov time, T_c , and the time for a close encounter with the perturber, T_c , applies. This relation, found empirically by Lecar et al (1992), predicts that T_c , is proportional to $T_l^{1.75}$.

Murray & Holman (1997) have explained this relation in terms of the Stochasticity Parameter, $K = (\pi\Delta\Lambda/\delta\Lambda)^2$, where $\Delta\Lambda$ is the width of the resonance and $\delta\Lambda$ is the separation between the resonances. If $\Delta K = K - K_c$, where K_c is the critical value (~ 1 , corresponding to the start of overlap), then they showed that $T_l \sim \Delta K^{-1.65}$ and $T_c \sim \Delta K^{-2.65}$, so $T_c \sim T_l^{1.6}$. This holds in the region of overlapping first-order resonances (the $\mu^{2/7}$ region). Orbits in this region show a range of more than three orders of magnitude in T_c . However, outside that region, they showed that the relation was in error by a factor of 10 at the 5:3 resonance (a second-order resonance), and by a factor of 100 at the 7:4 resonance (a third-order resonance). They also integrated 10 “clones” of Helga, an asteroid at the 12:7 resonance (a fifth-order resonance). Five of the clones had Lyapunov times ranging from 6,000 to 13,000 years. They encountered Jupiter in 1–4 Gyr (Gyr = 10^9 years). In this case the relation predicted $T_c \sim 6$ Myr (Myr = 10^6 years)—too low by a factor of 1,000. Murray & Holman (1997) showed that the mechanism for chaos in these higher order resonances was an overlap of the “subresonances,” and that diffusion between overlapping subresonances in the same mean-motion resonance is slower than diffusion between overlapping mean-motion resonances.

It is worth noting that higher order resonances become very narrow for zero eccentricity. For example, from Franklin et al (1984), the width of first-order resonances is proportional to $\mu^{2/3}$ for zero eccentricity. The corresponding widths of second-order resonances is proportional to μ and the width of third-order resonances is proportional to μ^2 . Thus, second and higher order resonances are

too narrow to overlap each other at low eccentricity. However, higher order resonances can occur in the wings of first-order resonances.

3 DYNAMICS IN THE ASTEROID BELT

Understanding the distribution of the asteroids as a function of their semimajor axes, and particularly where their mean-motions are commensurate with Jupiter's, provided dynamicists an intriguing puzzle for over 130 years—all the more so because these (Kirkwood) gaps occur at most mean-motion ratios, $n_A/n_{Jup} = p/q$, but a concentration of bodies at two others. Progress on this classic problem has been striking over the past 20 years. In a broad sense, it has been solved: We can identify the sources of orbital instability (or their absence) and the nature of their consequences and also have a good idea of some of the time scales involved. Numerical and analytic studies both have contributed extensively. Although several related dynamical processes have been—and still are—working to produce gaps in the asteroid distribution, the most significant ones can all be linked to the solar system's present environment. Carving gaps may in some cases require upwards of a billion years, but it can probably be done without requiring cosmogonic explanations; i.e. calling on processes that occurred in the primordial or developing solar system.

The paper that ignited the modern era of work on the Kirkwood problem was Jack Wisdom's (1982) first contribution to the study of the 3:1 mean-motion resonance at $a = 2.50$ AU. His startling results showed that an orbit at this resonance could remain quiescent, with a low eccentricity, $e < 0.1$, for more than 100,000 years but also show occasional surges lasting about 10,000 years that would lift e to a maximum value of about 0.35. Such a value is just sufficient to allow a

crossing of Mars' orbit, resulting in an eventual collision or a close encounter. Orbital computations as long as a million years were a rarity 20 years ago, and Wisdom's novel approach was to develop a mapping of the planar elliptic three-body problem that relied on two efficient techniques. The first approximated the short-period terms (i.e. ones characteristically arising during an orbital period) by a series of delta functions. The second averaged the Hamiltonian, expanded to second order in eccentricity, over the longer but still relatively short-term angular variable that librates at the 3:1 resonance.

In two following papers, Wisdom (1983, 1985) first used direct numerical integrations to verify the presence of the e_{max} peaks of 0.35 and, by including a third dimension, then showed that e_{max} could rise to $e = 0.6$, a value that also included Earth-crossing trajectories. At the same time he calculated the extent of the chaotic zone, showing that it closely matched the observed 3:1 gap width. The excitement generated by these results echoed widely: A straightforward dynamical process that (a) could open a gap at one resonance, (b) in principle might be generalized to account for other Kirkwood gaps, and as an added bonus, (c) could deliver asteroidal fragments into the inner solar system as meteorites, had at long last been identified. Later work by Ferraz-Mello & Klafke (1991) and Farinella et al (1994) showed that the chaotic zone at low e is linked, even in the planar elliptic three-body problem, to one with $e > 0.6$ so that $e \rightarrow 1$ can occur.

The panels of Figure 1 provide a quick insight into the chaotic behavior that Wisdom discovered at 3:1. Figure 1a plots the motion of both Jupiter's apsidal line, ϖ_J , and that of a low eccentricity body [$e_o = 0.05$] in the 3:1 resonance, and Figure 1b shows that the eccentricity surges occur when the two ϖ 's are approximately equal—in fact, $\varpi_A > \varpi_J$ corresponds to the rise in e . The equality

of two apsidal or nodal rates is referred to in solar system studies as an example of secular resonance. Their importance at certain locations in the asteroid belt has long been recognized (cf Brouwer & Clemence 1961), but only in the past decade has their role within mean-motion resonances been appreciated. Perturbations arising at mean-motion resonances will markedly effect the elements of bodies lying in them—yielding a very broad range of apsidal and nodal rates that are functions of e and i . The apsidal and nodal motion of the Jupiter-Saturn system is defined to high precision by two apsidal and one nodal terms that have been labeled ν_5 , ν_6 , and ν_{16} by Williams (1969). Figure 1a shows that the apsidal motion of a body with $a_0 = 0.481$ and $e_0 = 0.05$, which librates in the 3:1 resonance, will intermittently also resonate with the frequency of ν_5 and possibly ν_6 as well.

The challenge to map the locations and limits of the secular resonances that lie within the confines of many significant mean-motion resonances has been met on theoretical grounds in papers by Moons & Morbidelli (1995 and its references). Although this work concentrates on the planar case in which only ν_5 and ν_6 are present, it contains the important result that, in the higher order resonances, 3:1, 5:2, and 7:3, the ν_5 and ν_6 secular resonances exist over a very wide and overlapping range of a and e —to such an extent that a condition of widespread chaos is present inside these three mean-motion resonances. Figure 2 is a sample of their work for the 5:2 resonance.

The picture developed by Moons & Morbidelli (1995) provided one reason that led Gladman et al (1997) to study the fates of a large number of bodies placed in various mean-motion resonances. In a real sense their paper represents an elaboration and even a culmination of Wisdom’s original suggestion that marked

eccentricity increases are responsible for the Kirkwood gaps. Some eccentricity increases beyond the value of 0.35 found by Wisdom had already been noted, but Gladman et al provided accurate statistics by integrating more than 1000 bodies sprinkled throughout 3:1, about 450 in 5:2, and 150 each in 7:3, 8:3, and 9:4. Their study quantitatively describes the dynamical transfer process noted earlier by Wisdom (1983)—namely that gravitational encounters even with the terrestrial planets can provide sufficient energy changes to move bodies from regular to chaotic zones and even from one resonance to another. We can now legitimately claim that the development of a gap [cf Figure 3] at 3:1 is inevitable, though some details are complex and different time scales are followed. The next two paragraphs provide an outline of the process.

First, for bodies once in 3:1 with $e < 0.25$, the effect of imbedded secular resonances, principally ν_6 , will drive e 's of any and all bodies toward unity, leading most likely to solar impacts in times of a few million years. In the survey, this was the fate of about 70% of the initial population. A quarter to a third of them directly impacted the Sun, whereas the majority were gravitationally scattered by the Earth or Venus before doing so. Most of the remaining 30% moved in unstable orbits exterior to Saturn.

Second, the same fate awaits bodies of any eccentricity whose critical arguments are either circulating or that have librations greater than about 50° . However, bodies with $e > 0.3$ and that show small librations have different outcomes. In preparing for this review, we identified orbits of bodies with $0.3 < e < 0.6$, whose moderate librations, all $< 40^\circ$ qualified them as stable librating members of the 3:1 resonance. These orbits are regular; i.e. there is no sign of any exponential growth in their angular orbital elements during integrations lasting as long as 10^7

yr. Figure 4*a–c* is an example of one of them. Three (of three) remained in regular orbits until the integrations were terminated after 2 billion years. However, the eccentricities of all three of these “stable” orbits regularly climbed at least to 0.5, hence risking the gravitational encounters (or, less probably, actual collisions) with Mars mentioned above. (Mars itself was not included in these integrations.) Gladman et al found that 5% of all bodies initially in 3:1 were “extracted by Mars,” meaning that their orbits were first perturbed by Mars by a sufficient amount that the final result after subsequent encounters was most likely a solar impact or an orbit beyond Saturn. This seems the certain fate of the otherwise stable high eccentricity bodies—“otherwise” meaning the case with only Jupiter and Saturn present. Their result argues that this phase of the depopulation of 3:1 will require longer times, 10–100 Myr (with a tiny handful remaining after 100 Myr, but the eventual outcome is the same as that of their lower eccentricity neighbors. We can conclude that 3:1 is a resonance that has been emptied of any asteroids initially present by a natural, multi-stage dynamical process in which all planets, Venus through Saturn, have contributed.

The 5:2 resonance, although one order weaker than 3:1, behaves similarly but with some interesting differences. As was the case at 3:1, values of the eccentricity set three regimes: (*a*) Orbits of low e are severely chaotic owing to the influence of ν_6 . This remark applies to all bodies with $a \simeq a_{5:2} = 2.78$ AU and all $e < 0.2$. Figure 5*a–d* presents an example. (*b*) for $0.2 < e < 0.40$, orbits are regular, provided that their libration amplitudes are less than 11° and (*c*) for all larger e 's, orbits at least occasionally lie in secular resonance and are very chaotic with e 's reaching values > 0.7 . These remarks emphasize the resemblance to 3:1, but there are two novel features for bodies in the second category.

First, their e ranges generally do not include a close approach to Mars and second, as figures 5*c,d* show, in just one of many cases, the presence of secular resonance does not always correspond to extreme chaos. Taken together, figures 5*a-d* are examples of the differing response of two bodies at the 5:2 mean-motion resonance to secular resonances. When the amplitude of $\varpi_A - \varpi_J$ is large or when there is coincidence of the periods of the ν_6 term with the ϖ_A oscillations, then chaos is severe and is measured by Lyapunov times of ~ 1000 Jovian periods. By contrast, when the oscillations of ϖ_A no longer match the frequency of ν_6 and/or their amplitude is small the orbits remain regular. A tentative conclusion is that ν_5 is far weaker than ν_6 . Thanks to Moons & Morbidelli (1995) we have an accurate knowledge of the locations of the secular resonances as well as the limits on the orbital elements over which they operate. What we lack is an evaluation of their strength —say, a measure of the chaos they can produce within a mean-motion resonance. Murray & Holman (1997) have developed the means to calculate Lyapunov times when mean-motion resonances overlap. A related formalism applying to the case when secular and mean-motion resonances overlap would be very valuable.

In their study Gladman et al found that the loss of bodies from 5:2 closely resembled the depletion at 3:1; i.e. all objects were removed within 100 Myr. Our suggestion is otherwise: We expect a number of librating bodies with $e < 0.40$ to remain, unless a slow diffusion into the chaotic region has removed them all. However, there may not be a real conflict. Gladman et al were especially interested in the role of the 5:2 in delivering members of three nearby asteroid families into the inner solar system and hence chose initial velocity distributions accordingly. Inclusion of librators in such a distribution is very unlikely. By

contrast, their survey at 3:1, though it also followed the evolution of members of three families, introduced 1000 randomly selected orbits as well. The files of the Minor Center list some 30 possible candidates in the above eccentricity range at 5:2. Whether they do librate with small amplitudes and avoid secular effects is at present unknown.

Moons & Morbidelli (1995) have also mapped the one (weaker) secular resonance, ν_5 , that lies within the 4:1 mean-motion resonance, but 4:1 itself is unimportant because its semimajor happens nearly to coincide with the locations of the far stronger ν_6 and ν_{16} secular resonances that, independently of any mean-motion resonance, are now known to be the agents defining the inner edge of the asteroid belt at 2.1 AU.

Both Moons & Morbidelli (1995) and Gladman et al (1997) also examined the 7:3 mean-motion resonance. The former paper again shows that both ν_5 and ν_6 are centrally situated within 7:3 and cover large portions of it, both as $e \rightarrow 0$ and at e as high as 0.65 as well. In preparing for this review, we randomly introduced 120 bodies into the resonance and found severe chaos ($T_l < 2000P_J$) everywhere. Gladman et al (1997) found that depletion at 7:3 proceeds at a slower rate than at 5:2, with nearly one half of its initial bodies surviving to their integration limit of 40 Myr. Our results are roughly compatible with theirs but suggest a depletion rate that is faster by a factor of at least two. In any event, as Figure 3 attests and both results predict, 7:3 should be a genuine, fully developed gap, not just a region of reduced population.

The fifth-order resonances, 8:3 ($a = 2.71$ AU) and 9:4 ($a = 3.03$ AU) were not examined in the otherwise comprehensive studies of Moons & Morbidelli so we have introduced about 50 bodies in each to have some idea where chaos is most

important. The results contain few surprises: at 8:3 orbits with $e_p < 0.19$ are severely chaotic, with T_l 's $< 2000P_J$. In the range $0.19 < e_p < 0.35$ they are quite regular, having $\log T_l > 4.5$ (Jovian periods). They become increasingly chaotic at higher e 's, a fact that is of little importance because $e = 0.4$ leads to a Mars encounter. At 9:4 orbits are again very chaotic for $e_p < 0.2$ and much less so for $0.2 < e_p < 0.32$. Still, their average T_l 's are shorter by a factor of about three than those at 8:3. Eccentricities > 0.32 are again very chaotic, and those with $e > 0.45$ will be Mars crossers. Gladman et al (1997) found incomplete depletion at both 8:3 and 9:4, with about one half of the original population surviving after 40 Myr in the former and three quarters after 120 Myr at the latter. All of these estimates are qualitatively in accord with the distribution shown in Figure 3. [A likely interaction between 9:4 and 11:5 (3.08 AU) probably accounts for the extra width.] Longer surveys, with an eye to further quantifying diffusion rates into chaotic areas, are an important future project.

3.1 Chaos in the Outer Belt

The 2:1 resonance at 3.28 AU divides the populous inner belt from the much less dense outer portion [cf Figure 3]. Can it be that the entire outer belt is systematically more chaotic than the inner belt? The answer is certainly yes, and it has recently become possible to evaluate both its extent and severity throughout all of the outer belt where Holman & Murray (1996) have, among other results, shown that 22 of 25 outer belt minor planets have Lyapunov times shorter than $6000P_J$. However, it is also important to stress that there is more chaos in the inner belt than what we have thus far mentioned. Independent studies by Murray et al (1998) and Nesvorný & Morbidelli (1998) point out

that many three-body mean-motion resonances (cf Aksnes 1988), involving the longitudes of Saturn as well as Jupiter and the asteroid, are a major source of chaos. Nesvorný and Morbidelli (1998) trace the chaos in the orbits of about 250 of just the numbered minor planets to three-body resonances, finding Lyapunov times that lie in the range of 1,000 to 10,000 P_J . As the authors demonstrate, these resonances are vastly more dense in the outer belt, where their effect can only be more destabilizing.

Holman & Murray (1996) and Murray & Holman (1997) have studied chaos in the outer belt by examining orbital behavior at a number of high-order resonances (e.g. 12:7) where they have calculated both Lyapunov and diffusion time scales, analytically as well as numerically, and some escape times for comparison. They associate chaos with the overlap between members of individual mean-motion resonances. Consider the example of 12:7. In the planar case it is composed of six (sub)resonances, with various multiples of the two apsidal longitudes, e.g.

$$\sigma_k = 12\lambda_J - 7\lambda_A - k\varpi_A + (k - 5)\varpi_J, \quad (9)$$

for $k = 0, 1, \dots, 5$ and where the λ 's and ϖ 's refer to mean and apsidal longitudes. Two components, defined e.g. by k and $k+1$ can overlap and Holman & Murray (1996), having obtained their locations and widths, showed that their overlap will generate chaos. This approach to analyzing chaos within a given mean-motion resonance is the mathematical equivalent of the one used by Moons & Morbidelli (1995), who consider the overlap between a resonance defined by $\sigma(k)$ in Equation 9 and the secular one given by

$$\sigma_{secular} \equiv \varpi_A - \varpi_J = [\sigma(k + 1) - \sigma(k)]. \quad (10)$$

The latter is the approach taken by Wisdom in his analysis of the 3:1 resonance

(Wisdom 1985). In this approach it is sometimes assumed that there is an adequate separation between the time scales associated with $\sigma(k)$ and $\sigma(\text{secular})$ so that the action associated with $\sigma(k)$ is adiabatically preserved, except when the orbit is near the separatrix. However, these time scales are not adequately separated for most resonances in the asteroid belt.

Figure 6 plots some of Holman & Murray's results, indicating that (a) asteroids in the outer belt have already been ejected from resonances of order less than 4 (with the exception of 11:7), thus demonstrating that less well-defined Kirkwood gaps will also exist there; (b) escape times from fifth-order resonances correspond roughly to the solar system's age' and (c) objects in sixth-order resonances are ejected in times as long as 10^{11-12} years. We encounter again the problem discussed elsewhere in this review: Lyapunov times are measured in a few thousand P_J , but at least some of the carefully evaluated escape times exceed the age of the solar system. In view of these long times for ejection, it seems likely that other processes have contributed to the removal of some resonant and many non-resonant bodies from the extended outer belt. Holman & Murray (1996), Liou & Malhotra (1997), and Nesvorný & Ferraz-Mello (1997) have directed attention to planetary migration as a mechanism that will move various resonances into and through the outer belt, a process that can have further dynamical consequences, as the latter paper stresses, if there is also a change in the near 5:2 commensurability in the mean motions of Jupiter and Saturn. Lecar & Franklin (1997) and Franklin & Lecar (2000) have quantitatively studied the sweeping of secular resonances associated with the decay of the solar nebula through the asteroid belt. These papers show that this one mechanism can accomplish three desired ends: (a) remove an overwhelming fraction of an initial population from the outer belt,

(*b*) deplete the inner belt from a likely early value by a factor of about 1000 so as to match present observations, and (*c*) generate a range of eccentricities that are characteristic of the known minor planets. Their study also included gas drag on the asteroids.

3.2 Behavior at First-Order Mean-Motion Resonances

We turn at last to the behavior at two first-order resonances that Morbidelli & Moons once called the “most mysterious ones,” beginning with a discussion of the reason(s) for the pronounced gap at the 2:1 resonance, $a_0 = 0.630$ and the concentration of minor planets at the 3:2 resonance, $a_0 = 0.763$. Part but not all of this mystery has been dispelled as models have become more realistic. To be more precise, unless models include Jupiter and Saturn in eccentric precessing ellipses, they can not capture enough physics to account for the behavior at the first-order mean-motion resonances. The importance of secular resonance in developing chaos within such higher order mean-motion resonances as 3:1 and 5:2 might lead to the expectation that they should also be of prime importance here as well. However, a detailed mapping (Morbidelli & Moons 1993) shows that the role of ν_5 and ν_6 for generating chaos in the heart of both the 2:1 and 3:2 resonances applies only for orbits having eccentricities $e > 0.45$ and 0.25, respectively. The reason is clear enough: At low e 's, first order resonances drive pericentric longitudes, ϖ_A , much more rapidly than the motion of even the faster of the two principal terms (i.e. ν_6) that measure ϖ_J —by a factor of about 30 for orbits with e 's averaging about 0.15. We must look elsewhere for other resonances whose overlap at orbits of low e with the 2:1 resonance itself is the source of the chaos shown in figure 7*a*.

The ones we are looking for involve commensurabilities between multiples of the (resonant) libration and apsidal frequencies. The former are defined by the regular oscillations of the appropriate critical angle σ similar to Equation 9. Strictly periodic solutions have $\sigma = 0$; real bodies at mean-motion resonances show oscillations in σ with well-defined periods and amplitudes that also correspond to regular variations in their orbital elements, especially semimajor axis and eccentricity. Periods of σ increase with e , and at 2:1 and 3:2, typically lie in the range of 15 to 75 P_J , where P_J , the orbital period of Jupiter, is 11.86 years. Apsidal periods also depend on e , from close to $15P_J$ for very small values, then increasing rapidly. Therefore, a series of commensurabilities, starting near unity, which we label P_{apse}/P_{lib} in Figures 7 and 8 must occur.

Giffen (1973) first called attention to these commensurabilities, though their link to chaos was not stressed. Henrard and colleagues (cf Henrard and Lemaitre 1986, Lemaitre & Henrard 1990) first recognized their importance and began to investigate them analytically, and Franklin (1994, 1996), numerically. Following Henrard we shall refer to the small integer commensurabilities of P_{apse}/P_{lib} as secondary resonances. We can explore their behavior and importance by considering the planar example shown in Figure 7a–c. The figure shows that they are indeed the source of chaos within the 2:1 resonance by presenting three cases in which the two perturbers, Jupiter and Saturn, move in planar precessing orbits with (case a) their present eccentricities ($e_J = 0.044 \pm 0.016$; $e_S = 0.047 \pm 0.035$), then with one half (case b) and finally one tenth (case c) of these values. This sequence helps verify the claim that secondary resonances are responsible for chaos among (hypothetical) resonant asteroidal orbits of low eccentricity. [A slash, e.g. 5/3, denotes a secondary resonance, while a colon, e.g. 3:2, denotes a mean-

motion resonance.] Figure 7c shows that only the strongest secondary resonances are present and their widths are very narrow, but in figure 7a when $e(J)$ and $e(S)$ have normal values, higher order secondary resonances [e.g. 5/3] have also been excited and/or first-order ones have broadened so that extensive overlap occurs.

A quick interpretation of figure 7 might suggest that secondary resonances are the source of chaos in the entire range, $0 < e < 0.28$. If this is truly the case, then ones as high as 15/1 must still be contributing. Despite our present ignorance of their strengths, this in itself seems curious, though since P_{apse} is a rapidly rising function of $e(\text{asteroid})$, whereas P_{lib} is almost constant, it is also true that higher order resonances crowd closer and closer together. The fact that exactly at some weaker secondary resonances very regular orbits exist is also curious, though helpful, as it speeds the process of locating them. A supplementary explanation for chaos near $e = 0.2$ has been mentioned by Morbidelli & Moons (1993), who found that the ν_{16} secular resonance is present in the limit as $i \rightarrow 0$ and should affect orbits with $e = 0.21 + 0.04/ - 0.02$. However, the calculations leading to figure 7 are strictly limited to the planar approximation so that the origin of chaos for $e_0 < 0.15$ is clearly the province of secondary resonances, but to what e they extend is less clear.

Recently, Moons et al (1998) broadened this topic by mapping the locations of chaotic zones that arise from all secular and families of secondary resonances at inclinations of 0, 10, 20, and 30°. [As Henrard (1990) noted, secondary resonances are not confined to the case defined by $\dot{\sigma} = \dot{\varpi}_A$, but can include linear combinations of $\dot{\varpi}_A$ with the frequencies of planetary apsidal and nodal motion.] What is striking is the connected nature of the chaotic zones, extending through much of the area in the a, e plane for all four i 's. Depending on the inclination, one to

three islands are present that contain quite regular orbits, having $0.2 < e < 0.45$, many of which are not at risk because their perihelia avoid crossing Mars' orbit. Moons et al note that one of them is populated by five recently discovered minor planets, but the others are seemingly empty.

With the source of chaos identified, the question now turns to how the depletion of a hypothetical early population of bodies at 2:1 might have proceeded. This topic rests on less firm ground. Two independent sets of long-term integrations argue that objects with Lyapunov times as short as several hundred Jovian periods (a few thousand years) cannot permanently exist at 2:1. Franklin (1996) found examples of escape for single representative bodies placed in the 2/1, 3/1 and 5/1 secondary resonances, all after times close to 800 Myr. Objects in much higher secondary resonances, consequently with Lyapunov times three orders longer, remained after 4 Gyr. These integrations included only Jupiter and Saturn, which moved in planar precessing orbits. In five cases of escape orbital eccentricities rose to values that guaranteed a crossing of Mars' orbit only a few million years prior to escape, leading to the conclusion that drifting out of resonance, not an eventual encounter with Mars, is responsible for depopulating the region. At the same time Morbidelli (1996) reached a somewhat different conclusion, though one still compatible with the existence of a gap. His 3-dimensional integrations of 10 orbits with $0.055 < e < 0.155$ indicated that all became Mars crossers in times between 10 and 100 Myr. (His integrations were terminated once this orbit crossing was noted.) The same fate happened to most orbits with higher e 's, though four remained for a full 10^9 years. Most objects remaining at that time showed strong evidence that their proper eccentricities were diffusing toward higher values.

The more rapid crossing times found by Morbidelli may be the consequence of adding the third dimension to the problem. In a parallel development Henrard et al (1995) showed analytically that a strong (nodal) secular resonance overlaps several secondary resonances. They suggested that it may be possible for a body initially in a low e secondary resonance to diffuse or random walk with an increasing libration amplitude so as to enter the extensive field of principally nodal secular resonances that lie at much larger e 's and i 's. Their short integration times of only 1 Myr failed to provide an example. At this point in our discussion the 1998 paper of Moons et al assumes special importance because it indicates that the chaotic areas arising from various sources are not isolated islands, but are connected. Bodies may therefore diffuse from low to high eccentricity and escape with only small changes in semimajor axis, much as was found in the numerical study just mentioned. How and when these three islands, located by Moons et al (1998) and containing very regular orbits, have lost bodies is, despite Morbidelli's long integrations, still an unsolved problem. We would argue for additional very long term studies to quantify the process of diffusion especially for orbits with small-to-moderate librations in the $0.2 < e < 0.45$ range before placing all hope in an explanation linked to planetary migration (cf Nesvorný & Ferraz-Mello 1997). Despite our present state of uncertainty, there is now a general conviction that strictly dynamical effects linked to Jupiter and Saturn in their present orbits are still the best bet to exhaust a primordial population of bodies at the 2:1 resonance, but that such processes needed more than a billion years to yield the current minor planet distribution.

Figures 8*a,b,c*, the companion to Figures 7*a,b,c*, present parallel results for the 3:2 mean-motion resonance, which is characterized not by a broad gap but

by a concentration of nearly 200 bodies (called the Hilda group) in reliable (i.e. observed for two or more oppositions) librating orbits. The difference in the observed appearance at the two resonances is clearly reflected in their dynamical behavior. Although the strongest secondary resonance at $P_{apse}/P_{lib} = 2/1$ is easily identified in Figure 8, it is less deep (less chaotic) and far narrower than is the case at 2:1. Even when the eccentricities of Jupiter and Saturn are doubled (cf. Figure 8 c) its width is far less than its counterpart at 2:1. A notable feature of the Hildas is the absence of bodies with proper eccentricities, $e_p \lesssim 0.10$. Figure 8a shows that chaotic orbits dominate in the region $e_0 \simeq e_p < 0.05$ and that a mix of chaotic and regular ones lie from $e_0 = 0.05$ to the 2/1 secondary resonance at $e_0 = 0.074$ with regular ones alone present at higher e_0 's, except exactly at other secondary resonances.

Nesvorný & Ferraz-Mello (1997) have compared the long-term behavior throughout the 2:1 and 3:2 resonances. Their approach applies the frequency map technique discussed by Laskar (1993) to determine the diffusion of (Fourier) frequency components in a resonant body's pericentric motion. The results show that all orbits in the heart of the 3:2 with $0.05 < e < 0.35$ diffuse very slowly, with percentage frequency shifts of about 10% in a billion years. At 2:1 the broad, continuous region found at 3:2 is replaced by numerous smaller islands also having slow diffusion, but they are surrounded by a sea of orbits where diffusion is some 10 times faster. These plots are compatible with surveys providing Lyapunov times, but they are quicker to obtain and hence more complete. By either criterion, however, disruptive processes are one to two orders more severe and/or more effective over wider ranges of semimajor axis and eccentricity at 2:1. Efforts along these lines imply that the population difference between these two

resonances is principally a matter of time scale: Wait long enough and the Hildas too will probably disappear, leaving behind a sort of undefined Kirkwood Gap at 3:2. We have integrated orbits of 10 hypothetical bodies with $0.02 < e_0 < 0.075$ over the age of the solar system and found no signs of escape, but these integrations were only 2-dimensional. Longer integrations in three dimensions are a useful topic to pursue. However, it is hard to rest content with present and future population statistics alone. We would like understanding at a still more fundamental level: Why is the core of 3:2 not broken into islands the way 2:1 is and, the related question, why are Henrard's secondary resonances so much weaker there? Perhaps the latter are a good starting point for future work. Henrard's studies have located many of them as functions of eccentricity and inclination only within the 2:1 resonance, but their relative and absolute strengths have yet to be calculated. Despite much progress we do not yet understand the ultimate reason for their curious behavior that is strong enough to produce marked chaos at 2:1 over all a and $e < 0.25$, but only in narrow slices at 3:2.

The recent literature on the Kirkwood problem is extensive. For those interested in more details, we recommend papers by Wisdom, Henrard and colleagues, Morbidelli, Moons and colleagues, Holman & Murray (1996) and a review by the late Michele Moons (1997).

4 LONG-TERM STABILITY OF SMALL BODIES IN THE OUTER SOLAR SYSTEM

A vast number of asteroids occupy the region between Mars and Jupiter, and an even larger number of Kuiper belt objects exist near and beyond Neptune. Nevertheless, these objects contribute very little to the total mass of the solar

system. The main asteroid belt and Trojan asteroids are estimated to contain a total of $\sim 10^{24} - 10^{25}$ grams and the Kuiper belt no more than an Earth mass of material. In comparison to the mass of the planets themselves, this additional mass is almost negligible. In this sense, the regions between the planets are remarkably empty. Is this scarcity of material the result of particular processes of planet formation? That is, were those processes so efficient that nearly all of the initial mass was either incorporated into planets or swept away? Alternatively, are the gravitational perturbations of the present planets sufficient to eject nearly all of the material initially between the planets on time scales less than the age of the solar system?

Of course, these two ideas are not independent. The gravitational perturbations from proto-planets constitute one of the main physical processes during planet formation. The presence of proto-planets influences the orbital distribution of planetesimals that may or may not be accreted. Given the broad range of relevant physical processes and the computational challenge of including a sufficient number of bodies, direct simulations of planet formation are still severely limited.

It is much more straightforward to evaluate the gravitational influence of the present planetary system on smaller bodies. As we will see, the perturbations of the present day planets are sufficient to eject nearly all material from between the planets on time scales less than the age of the solar system. However, one cannot conclude that no other important physical process contributed to the absence of material between the planets. We will also see that there are regions in the solar system in which the time scale for removal by gravitational perturbations alone exceeds the age of the solar system. We will find dynamically long-lived regions

that are empty of material, long-lived regions in which the orbital distribution appears excited by perturbations of bodies that are no longer present, and regions with dynamical life times that straddle the age of the solar system. It is in these regions that simulations of the long-term dynamics provide the richest evidence of the conditions of planet formation. In the following sections we discuss recent results on the long-term stability of small bodies in the regions between outer and inner planets.

4.1 The Region between Jupiter and Saturn

The abrupt decrease in the surface density of asteroids beyond the 2:1 mean-motion (near 3.3 AU) revealed by the Palomar-Leiden Survey (van Houten et al 1970) prompted Lecar & Franklin (1973) to study numerically the possibility that there were initially asteroids beyond where they are presently found. In addition to examining the long-term stability of small bodies in the outer asteroid belt, they examined the stability of such objects between Jupiter and Saturn. Modeling Jupiter and Saturn as moving on fixed elliptical orbits and considering the planar case, they integrated 100 test particles started on orbits between 5.7 and 9.1 AU with eccentricities between 0.0 and 0.1. After numerically integrating for 500 Jupiter periods (~ 6000 years), only test particles near 6.8 and 7.5 AU remained. The others escaped. Lecar & Franklin (1973) cautiously concluded that the Jupiter-Saturn region would be depleted of asteroids in a few thousand years, with the possible exception of the two identified bands. Everhart (1973), in an independent study, identified the same long-lived bands in integrations lasting 3000 Jupiter periods. He then selected one test particle from each band and numerically integrated them until their orbits behaved chaotically (7,100 and

17,000 Jupiter periods, respectively).

Franklin et al (1989) reexamined this problem, armed with faster computers that would permit longer numerical integrations. Although again the planar problem was considered, the effect of the mutual gravitation of the planets was modeled according to the leading two terms of the secular theory (see Murray & Dermott 1999). The authors chose planet crossing orbits as their criterion for stopping a test particle integration. That is, if the test particle crossed the orbit of Jupiter or Saturn it was said to be ejected. Of the 135 test particle orbits integrated between Jupiter and Saturn, none survived. The longest lived was ejected after 799,000 Jupiter periods (9.4×10^6 years). The authors concluded that low-eccentricity, low-inclination orbits between Jupiter and Saturn were unlikely to survive longer than 10^7 years. In addition to being the first to determine the full range of dynamical lifetimes of test particles between Jupiter and Saturn, the authors found that all orbits displayed a positive Lyapunov exponent (were chaotic) before ejection.

Soper et al (1990) extended this work to find a correlation between the estimated Lyapunov times and the ejection times of the test particles between Jupiter and Saturn. In addition, they established that their results were not sensitively dependent upon the numerical accuracy of the integrations. Even for dramatically degraded accuracy, stable orbits in the circular restricted three-body problem remain stable.

Weibel et al (1990) also reexamined the problem of stability between Jupiter and Saturn. The principal improvements of their work over previous studies were to integrate the actual orbits of Jupiter and Saturn and to integrate the full three-dimensional problem. Studying a sample of 125 test particles with initially

low-eccentricity, low-inclination orbits, they found that nearly all were planet crossing or ejected within 20,000 years, with a small number surviving more than 10^5 years, in agreement with other results. Weibel et al (1990) also associated some of the variation in dynamical lifetime with the locations of mean-motion resonance with Jupiter or Saturn.

4.2 The Regions Between the Other Outer Planets

As in the case of the outer asteroid belt and the region between Jupiter and Saturn, the question of whether there are regions in the outer planet region where small bodies might be stable on time scales of 10^9 years has been raised numerous times in the literature. This question has been investigated by several groups using a variety of techniques.

Duncan et al (1989) developed an algebraic mapping to approximate the motion of a test particle orbiting between two planets. The mapping is composed of a part that follows the motion between conjunctions with a planet and a part that includes the impulsive gravitational influence at conjunction. Although the assumptions required to make its development tractable are severe, the mapping nevertheless recovered the size of the chaotic zone near a planet (Wisdom 1980) and the instability of test particles between Jupiter and Saturn. This mapping's speed relative to direct numerical integration permitted simulations lasting of order 10^9 years, well beyond what could be completed at the time with available computers and conventional algorithms. With their mapping, the authors identified bands of long-term stability between Saturn and Uranus, Uranus and Neptune, and beyond Neptune.

Gladman & Duncan (1990) were the first to complete accurate, direct numerical

integrations of test particles in the Saturn-Uranus and Uranus-Neptune regions and beyond Neptune, as well as in the outer asteroid belt and Jupiter-Saturn region. Although their integrations were limited to 22.5 Myr by computational speed, they followed the trajectories of roughly one thousand test particles. Their additional advance was to include the perturbations of the four mutually interacting giant planets as perturbers, integrating individual test particles until they entered the gravitational sphere of influence of one of the planets. In addition to finding a clearing in the outer asteroid belt associated with mean-motion resonances and short time-scale dynamical erosion just beyond Neptune, they found that the majority of test particles between the giant planets undergo close approaches with the planets in $10^5 - 10^7$ years. Whereas some test particles between each of the planets were found to survive, the authors noted that they did not expect them to be stable over the lifetime of the solar system.

Extending the work of Gladman & Duncan (1990), Holman & Wisdom (1993) studied test particle stability in the invariable plane from 5 to 50 AU. Placing a total of 3000 test particles in circular orbits in the invariable plane (500 test particle in each of 6 initial longitudes), they integrated the particles for up to 800 Myr interior to Neptune and 200 Myr exterior to Neptune. This was subsequently extended to 4.5 Gyr interior to Neptune and 1.0 Gyr exterior to Neptune by Holman (1995). The roughly order of magnitude speed-up in numerical integrations gained by the symplectic mapping method of Wisdom & Holman (1991) allowed the more complete study. Duncan & Quinn (1993), who approximated the motions of the outer planets by linear secular theory reported similar results.

Figure 9 displays the dynamical lifetime as a function of initial semimajor axis. The solid line marks the minimum survival time of the six test particles

initially in each semimajor axis bin. The encounter times of the test particles at the other initial longitudes for each semimajor axis bin are plotted as points, with surviving test particles plotted as open circles. A number of dynamical features are immediately apparent. In each semimajor bin there is a fairly broad range of dynamical lifetimes, sometimes two orders of magnitude. As noted above, between Jupiter and Saturn nearly all test particles are removed by $10^5 - 10^6$ years. Test particles between Saturn and Uranus are nearly all removed by 10^8 years, and those between Uranus and Neptune by 10^9 years. Other than test particles librating about the triangular Lagrange points of one of the planets and test particles beyond Neptune, only a single test particle survived.

As Holman (1997) demonstrated, even this one surviving test particle does not represent a stable region between Uranus and Neptune. In the region 24–27 AU a small fraction (0.3 per cent) of a population of initially low eccentricity, low inclination orbits will survive 4.5 Gyr. This region is long-lived but not indefinitely stable.

Recently, Grazier et al (1999a,b) revisited the issue of test particle stability in the Jupiter-Saturn, Saturn-Uranus, and Uranus-Neptune regions. They placed roughly 100,000 test particles in the Jupiter-Saturn zone and 10,000 test particles in each of the Saturn-Uranus and Uranus-Neptune zones. They employed a high-order linear multistep integrator with round-off error minimization and a small time step to accurately integrate their trajectories. Although their choice of initial orbital distributions makes direct comparisons difficult, their results largely confirm earlier ones and provide more detailed information of the time dependence of the removal of material as a function of orbital distribution.

4.3 The Inner Solar System

Although test particle stability in the outer solar system has been thoroughly studied by a number of groups, few corresponding studies of the inner solar system have been conducted. Mikkola & Innanen (1995) numerically integrated a few hundred test particles in the inner planet region (0.3–4.0 AU) for times up to 3 Myr. They included all the planets as perturbers. In addition, they estimated the Lyapunov times of each of the test particles by integrating the tangent equations of the Wisdom-Holman mapping (see Mikkola & Innanen 1999). Figure 10 shows these results. The test particle trajectories in the figure display a wide range of Lyapunov times, $10^2 - 10^6$ years. As Mikkola & Innanen (1995) point out, the longest Lyapunov times (least chaotic trajectories) are found in the vicinity of the main asteroid belt. Outside of the main asteroid belt most of the test particles developed large enough eccentricity in the course of the integrations to become planet crossing. Whereas not all planet-crossers were ejected in 3 Myr, the authors suggested that longer integrations would clear many of the remaining such objects. However, the authors did identify two narrow regions, one between Venus and Earth and one just beyond Earth, where one might expect to find long-lived asteroid orbits with low eccentricity and inclination.

Evans & Tabachnik (1999) integrated approximately one thousand test particles in the region 0.09–2.0 AU for times up to 100 Myr. They, like Mikkola & Innanen (1995), included the nine planets as perturbers. In addition, Evans & Tabachnik integrated five test particles at different initial longitudes in each semimajor axis bin to test the resulting range of dynamical lifetimes. Figure 11 shows the results of their study. On time scales of 100 Myr a large fraction of the objects were removed; however, long-lived regions can be seen. Evans &

Tabachnik (1999) fit logarithmic and power-law decay profiles to populations, extrapolating the surviving population to 5 Gyr. They found two regions that could possibly harbor dynamically long-lived populations, 0.09–0.21 AU (interior to Mercury) and 1.08–1.28 AU (between Earth and Mars). A few low-eccentricity and low-inclination asteroids in the latter region can be found in current asteroid catalogs.

4.4 The Kuiper Belt

Arguing that the surface density of primordial material in the solar system should not end abruptly beyond the outer planets, Edgeworth (1943, 1949) and Kuiper (1951) independently suggested that a disk of material might be found beyond Neptune. Edgeworth (1943, 1949), furthermore, proposed that such a disk might serve as a reservoir of short-period comets. Decades later, numerical investigations (Fernandez 1980, Duncan et al 1988, Quinn et al 1990) showed that the orbital distribution of short-period comets is more consistent with an origin in a flattened, extended disk than in an isotropic distribution such as the Oort cloud (Oort 1950).

The discovery of the first Kuiper belt object by Jewitt & Luu in 1992 (Jewitt & Luu 1993) and the subsequent discovery of nearly 400 such objects has transformed the study of the trans-Neptunian region from a purely theoretical endeavor to one that is observationally grounded. For a recent review of the physical and observational aspects of the Kuiper belt we direct the reader to the recent chapter by Jewitt & Luu (2000).

The study of the long-term dynamics of the Kuiper belt is a rapidly maturing field with a rich literature. We describe only research that pertains to the issue

of dynamical chaos. [For broader reviews of Kuiper belt dynamics see Morbidelli (1998) and Malhotra et al (2000). For a recent review of the formation and collisional evolution of the Kuiper belt see Farinella et al (2000)].

In the first numerical experiments to examine the importance of dynamical chaos in the Kuiper belt, Torbett & Smoluchowski (1990), improving upon the work of Torbett (1989), estimated the Lyapunov times of a large number of test particles with orbits beyond Neptune. Their 10 Myr integrations included the four giant planets moving on fixed ellipses as perturbers. They identified a large chaotic zone that roughly coincides with test particle perihelia between 30 and 45 AU. The Lyapunov times in this zone are less than 300,000 years. Torbett & Smoluchowski also noted that a small fraction of the test particles in this chaotic zone exhibit sizable diffusion throughout the zone. In addition, a fraction of the material in the belt could be scattered to large semimajor axis and effectively stored, forming a reservoir of comets.

Holman & Wisdom (1993) and Levison & Duncan (1993) directly demonstrated the viability of the Kuiper belt as a reservoir of short-period comets. Their numerical integrations showed a mixture of stable and unstable regions beyond Neptune. Small bodies in low eccentricity, low inclination orbits in some regions of the Kuiper belt can be delivered to Neptune-encounter orbits on time scales of $10^7 - 10^9$ years, with hints of instability on longer time scales (see Figure 9). Other regions appear stable for longer than 10^9 -year time scales. This is an essential point because an effective source of short-period comets must possess regions that are unstable on time scales comparable to the age of the solar system. Dynamical lifetimes significantly shorter than the age of the solar system would imply a now-depleted reservoir; a significantly longer dynamical time scale

would imply an inadequate supply of short-period comets. Indeed, detailed calculation of the dynamical evolution of small bodies upon exiting the Kuiper belt or its extended component demonstrate that it is the likely source of short-period comets (Levison & Duncan 1997, Duncan & Levison 1997).

Duncan et al (1995) improved upon this early work by mapping the dynamical lifetimes in the Kuiper belt for a range of semimajor axes, eccentricities, and inclinations. Figure 12 displays the principal results of this study. The long-lived region can be described as those semimajor axes and eccentricities that give perihelia greater than 35 AU, with the exception of an unstable band between 40 and 42 AU associated with the overlap of secular resonances (Knežević et al 1991, Morbidelli et al 1995). Although figure 12 reveals a rich dynamical structure, the underlying dynamics or causes of chaos and instability in the Kuiper belt were not explored in detail by Duncan et al (1995).

Two complementary approaches have been used to investigate the dynamical structure of the Kuiper belt. Morbidelli et al (1995) applied tools developed for the study of dynamics in the asteroid belt (Morbidelli & Moons 1993, Moons & Morbidelli 1995) to the Kuiper belt. Their approach was to use the planar circular restricted three-body problem, averaged for a particular resonance, to simplify the problem to a single degree of freedom. From that model the widths of a mean-motion resonance, in a semimajor axis, as a function of semimajor axis were computed. Morbidelli et al (1995) used similar models to examine the dynamics in secular resonances outside of mean-motion resonances. They pointed out that the unstable region 40–42 AU at low eccentricity and the large eccentricity excursions seen there by Holman & Wisdom (1993) result from the interaction of the ν_8 and the ν_{18} secular resonances. Likewise, in the region 35–36 AU large scale

chaos results from the interaction of the ν_7 and ν_8 secular resonances. The basic limitation of this approach, as the authors noted, is that each resonance must be examined in isolation to reduce the problem to a tractable single degree of freedom. Whereas these models can accurately describe the overall dynamics, the chaos that results from overlapping resonances is eliminated.

Malhotra (1996) used an alternative approach to map the boundaries of quasi-periodic regions associated with mean-motion resonances in the Kuiper belt. Surfaces of section of the circular restricted three-body problem show a divided phase space, with quasi-periodic regions interspersed with chaotic zones. Near a given mean-motion resonance the surfaces of section will show a stable island corresponding to the stable range of libration amplitudes or semimajor axis oscillation for a given eccentricity. Malhotra used the results from a series of surfaces of section to establish the stable boundaries of mean-motion resonances. These boundaries are somewhat narrower than those computed by Morbidelli et al (1995) because the analytic models can not account for the chaotic zones. Although the approach of using surfaces of section of the circular restricted three-body problem captures some the important effects of dynamical chaos at first-order mean-motion resonances, it also has a fundamental limitation. The eccentricity of Neptune's orbit must be ignored and only the planar case considered in order to reduce the problem to two degrees of freedom, from which a useful section can be computed. Thus, secular resonances from Neptune or other planets cannot be included. However, surfaces of section could be used to explore the dynamics in the regions of overlapping secular resonances in the Kuiper belt (see Šidlichovský 1990).

Aside from establishing the general framework of stability in the Kuiper belt,

the dynamical behavior in the 2:3 mean-motion resonance with Neptune has been studied extensively by a number of groups. This particular resonance has attracted a great deal of attention because, in addition to Pluto, a sizable population of Kuiper belt objects resides there. Whereas the orbit of Pluto and the resonances it occupies have been long established and well studied (see Malhotra & Williams 1997, the range of orbital parameters of the known Plutinos motivated broader studies of the 2:3 dynamics. Morbidelli (1997) examined the orbital diffusion throughout the resonance, finding dynamical lifetimes ranging from 10^6 years to times in excess of the age of the solar system. In addition, Morbidelli (1997) studied the role played by the ν_8 and ν_{18} secular resonance and the Kozai resonance within the 2:3 mean-motion resonance libration region. Related work on the dynamics in this resonance has been reported by Gallardo & Ferraz-Mello (1998) and Yu & Tremaine (1999) The importance of dynamical scattering among different members of the 2:3 resonance has also been recently examined by a number of groups (Ip & Fernandez 1997, Yu & Tremaine 1999, Nesvorný et al 2000).

Although other Kuiper belt mean-motion resonances have not been studied with as much detail as has the 2:3, the whole suite of resonances plays an important role in determining the overall structure and extent of the belt. The discovery of the first scattered disk object, 1996 TL66, along with the recognition that the population of such objects must be substantial (Luu et al 1997), confirmed the suggestion of Torbett & Smoluchowski (1990) that scattered Kuiper belt objects could be effectively stored at great heliocentric distances. Independent work by Duncan & Levison (1997) at the time of this discovery immediately demonstrated by long-term numerical integration the mechanism of this storage. As a

Kuiper belt object begins to undergo close approaches to Neptune, presumably after developing a large eccentricity in an unstable but long-lived region of the belt, the object's orbit follows a modified random walk. Successive encounters with Neptune alter the semimajor axis and eccentricity of the object's orbit in a way that roughly preserves perihelion distance (which is near Neptune). As a resonant value of the semimajor axis is approached, the random walk is altered. In some cases, as Duncan & Levison (1997) demonstrate, temporary resonant trapping occurs, sometimes with a reduction in eccentricity that raises the perihelion distance beyond the immediate influence of Neptune. This effect was first discussed by Holman & Wisdom (1993). These orbits, although trapped for very long times, will eventually develop large enough eccentricities to begin encountering Neptune again. By this means the scattered disk serves as an effective reservoir. It is clear that all of the trajectories that exhibit long-term capture in resonance are chaotic despite being long-lived. Although numerical integrations have demonstrated this, there is little analytic work on the details of this capture. Such work would provide valuable insight into how material in the extended Kuiper belt is distributed.

5 PLANETARY CHAOS

5.1 Numerical Integrations

By the 1980s it was clear that most Hamiltonian systems exhibited both chaotic and regular (on tori) motion. The chaotic motion is intimately tangled up with regular motion on KAM tori. However, the prevailing feeling was that the solar system was almost certain to lie on a KAM torus.

This expectation seemed to be supported by early attempts at accurate long

term integrations of the solar system, including those of Applegate et al (1986), who carried out integrations over 3 Myr, neglecting Mercury. The LONGSTOP project integrated the outer solar system (Jupiter through Pluto) using a standard general purpose integrator for a time of 9.3 Myr (Milani et al 1986). In these and other integrations the planets did nothing untoward. Applegate et al also carried out 200 Myr integrations of the outer planets. The motion appeared to be multiply periodic, as expected of motion on KAM tori, although they noted the presence of very long period variations in Pluto's orbital elements.

It was therefore a surprise when Sussman & Wisdom (1988) showed that the orbit of Pluto was chaotic. They used a special purpose-built computer called the Digital Orrery, running a twelfth-order Stormer integrator. This work featured the first attempted measurement of the Lyapunov exponent of the planetary system. The Lyapunov exponent is a standard tool in the arsenal of nonlinear dynamics, designed specifically to see if a system is chaotic. If the separation grows exponentially with time, $d(t) \sim e^{t/T_l}$, the orbit is chaotic. Multiply periodic orbits lead to much slower power law separation with time, $d(t) \sim t^\alpha$. Sussman & Wisdom (1988) found that the orbit of Pluto was chaotic, with a Lyapunov time of $T_l \sim 20$ Myr. Later, the LONGSTOP integrations were extended (Nobili et al 1989). This paper did not examine Lyapunov times, but it suggested, based on the appearance of the Fourier spectrum, that the orbits of the outer planets might be chaotic.

At roughly the same time Laskar (1989) performed numerical integrations of a very different type of model. He solved a subset of Lagrange's equations for the orbital elements; Lagrange's equations are similar to Equation (5). Laskar's model consisted of analytically averaged equations describing the motion of all the

planets except Pluto. In this model he kept secular terms up to second order in the planetary masses and to fifth order in eccentricities and inclinations (Laskar 1985). He also included the analytically averaged secular effects of all mean motion terms up to the same order. This involves dropping any term exhibiting a sinusoidal function whose argument contains a mean longitude. However, it does account for the (secular) effects of terms proportional to the product of two such sinusoids. For example, consider Equations (5), (3), and (8). Every term in the disturbing function is proportional to M_2 . To lowest order in mass the simple averaging procedure employed consists of dropping every term in (3) that contains a mean longitude in the argument of cosine.

However, Laskar (1989) considered terms of second order in the masses. For example, consider using Equation (7) in an extended development of (5). The right hand side of the latter will contain a term proportional to

$$4a_1 \frac{a_1}{a_2} \frac{M_2}{M} \frac{n_1}{2n_1 - 5n_2 + 3\dot{\varpi}_1} \phi_{2,-5,3,0,0,0}(a_1, a_2) e_1^3 \cos[2\lambda_1 - 5\lambda_2 + 3\varpi_1] \\ \times - 2 \frac{\mathcal{G}M_2}{a_2} \phi_{2,-5,2,1,0,0}(a_1, a_2) e_1^2 e_2 \sin[2\lambda_1 - 5\lambda_2 + 2\varpi_1 + \varpi_2]. \quad (11)$$

Using the trigometric identity $\cos(a + b) \sin(a + c) = (1/2) \sin(2a + b + c) + (1/2) \sin(c - b)$, we see that this term will give rise to a factor $\sin(\varpi_2 - \varpi_1)$. Because neither λ_1 or λ_2 appear, this secular term contributes to the averaged Hamiltonian. Terms that are nearly resonant, i.e. terms in which the combination $pn_1 - qn_2$ are small, will produce relatively large (compared with the simple estimate M_2^2) contributions to the averaged Hamiltonian. Laskar's (1989) model contained some 150,000 secular and averaged terms.

Laskar (1989) found by numerical integration over 200 Myr that in his model the entire solar system was chaotic, with $T_l \approx 5$ Myr. He stated without explanation that "the chaotic behaviour of the Solar System comes mainly from the

secular resonances among the inner planets.”

In a later paper Laskar (1990) showed that two combinations of secular angles appeared to alternate between libration and rotation, implying that the orbit crossed the separatrix of these resonances. Such behavior is associated with chaotic motion; in certain cases it may be the origin of the chaos. However, the two resonances Laskar identified involved the angles $\sigma_1 \equiv (\varpi_1^0 - \varpi_5^0) - (\Omega_1^0 - \Omega_2^0)$ and $\sigma_2 \equiv 2(\varpi_4^0 - \varpi_3^0) - (\Omega_4^0 - \Omega_3^0)$. The angle ϖ_4^0 is associated with the fourth normal mode of the planetary eccentricities, with a similar interpretation for the other ϖ_0 's. In some instances (such as Jupiter) $\varpi_5 \approx \varpi_J$, but the ϖ 's are a combination of all the normal modes. Similarly the angle Ω_4^0 is the angle associated with the fourth normal mode of the planetary inclinations. Because the two resonances identified by Laskar do not interact directly, they are unlikely to produce any substantial chaos.

Because Laskar employed an averaged system of equations, it was important to verify his results using an unaveraged system of equations. This was done by Laskar et al (1992). They examined the numerical solution of Quinn et al, a 6 Myr integration of the entire solar system. Although this integration was not long enough to detect the chaos, it did allow them to verify that the resonant argument $2(\varpi_4^0 - \varpi_3^0) - (\Omega_4^0 - \Omega_3^0)$ alternately librated and rotated.

Two years later Laskar (1994) identified a second secular resonance involving Earth and Mars; $\sigma_3 \equiv (\varpi_4^0 - \varpi_3^0) - (\Omega_4^0 - \Omega_3^0)$. He noted that on some occasions σ_2 librated when σ_3 rotated, and vice versa. This led him to suggest that the overlap of these two resonances was responsible for the chaotic motion.

The next advance was the work of Sussman & Wisdom (1992). They employed the Wisdom-Holman symplectic mapping to perform a 100 Myr integration of

the entire solar system, which they found to be chaotic with $T_l \approx 5$ Myr. This type of integration accounts for all types of resonance, both secular and mean-motion. They confirmed that the first two resonances identified by Laskar (1989) do exhibit both libration and rotation, but the second Earth-Mars, σ_3 resonance never librated, but only rotated, in their integrations. They were careful to point out that this did not rule out the interpretation of Laskar that the two resonances involving Earth and Mars overlap to cause the chaos.

They also found two other combinations of angles that, in their integrations, both librate and rotate, namely $\sigma_4 \equiv 3(\varpi_4^0 - \varpi_3^0) - 2(\Omega_4^0 - \Omega_3^0)$ and $\sigma_5 \equiv (\varpi_1^0 - \varpi_8^0) + (\Omega_1^0 - \Omega_8^0)$. They found that four of the five angles (all but σ_3 showed a transition from libration to rotation, or vice versa, at roughly the same time). This strongly suggests to us that some, as yet unidentified, mechanism is forcing the transitions seen in the integrations. This point is reinforced by the observation that σ_1 and σ_2 do not strongly interact.

In addition to confirming Laskar's basic result that the entire solar system is chaotic, Sussman & Wisdom found that the outer planets by themselves were chaotic, with $T_l \approx 7$ Myr. The Lyapunov times found in their giant planet integrations seemed to depend on the step size, at first glance a rather disturbing finding. However, a second set of integrations using a general purpose Stormer scheme again showed that the system was chaotic, this time with $T_l \approx 19$ Myr.

As a check that some long-term integrations of a planetary system were not chaotic, they carried out a 250 Myr integration of the outer planets without Uranus and found no evidence of chaos.

These numerical experiments indicated that the solar system was chaotic, but there was no indication in any of the integrations that any of the planets would

suffer either ejection from the solar system or collision with another body. In this sense it appeared that the solar system was stable. This comforting interpretation was bolstered by a 25 Gyr integration carried out by Laskar (1994). He found that none of the planets (excluding Pluto, which was not integrated) suffered an ejection or collision over that time. This suggested that the solar system was stable for 10^{10} years or more.

Laskar's integration showed that the eccentricity of Mercury varied between 0.1 and 0.5, with an average value of about 0.2. He attributed the variations to a diffusive process, driven by chaos. If we assume that this is the case, we can estimate the diffusion coefficient, and hence the time to remove Mercury by collision with the sun or with Venus, when $e \rightarrow 1$. The diffusion coefficient is

$$D \approx (\bar{G} - \bar{G}_0)^2 / T, \quad (12)$$

where $\bar{G} \approx e^2/2$ and T is the length of the integration, 25 Gyr. We estimate the maximum excursion in \bar{G} using $e_0 = 0.2$ and $e = 0.5$, corresponding to $\bar{G}_0 = 2 \times 10^{-2}$ and $\bar{G} = 0.125$. We make the assumption that the diffusion coefficient is independent of e , which is incorrect but adequate for our purposes. We find $D \approx 1.5 \times 10^{-2} / T$. The time for e to diffuse to 1 is

$$\tau_{esc} \approx 1/D = T/1.5 \times 10^{-2}, \quad (13)$$

or about 2×10^3 Gyr, or 2×10^{13} years. Laskar then repeated the integrations several times, each time changing the eccentricity of Earth by about one part in a billion. The integrations differed in detail, but no collisions or ejections were seen.

One might question whether Mercury could actually diffuse to such a large eccentricity; might there be some dynamical barrier preventing it from doing so?

In a series of numerical experiments Laskar (1994) showed that there were indeed orbits in his averaged equations that were very close to those of the solar system, and for which Mercury suffered a collision with the sun. In his words, he “decided to guide Mercury to the exit.” He made four clones of the Earth’s averaged orbit, again changing the eccentricity by different amounts of the order of a part in a billion. He then integrated for 500 Myr. He retained the solution having the largest value of e for Mercury, using it to produce four more clones with altered orbits for Earth.

Repeating this process 18 times, Laskar found a system in which the pseudo-Mercury was ejected after a 6 Gyr integration. This is much shorter than our estimate above, but this is to be expected because Laskar was actively searching for the most unstable orbit. The significance of the experiment is not that it predicts loss of Mercury on times comparable to the age of the solar system; the earlier experiments had already shown that the time for this to occur was longer than 25 Gyr. Rather, the experiment showed that it was plausible that there were no dynamical barriers to the loss of Mercury due to chaotic perturbations.

Murray & Holman (1999) carried out roughly 1000 long-term integrations of the outer solar system using the Wisdom-Holman symplectic mapping. They investigated the effect of altering the semimajor axis a_U of Uranus, tracing out the variation of T_l as a function of a_U . Using this technique, they located chaotic regions associated with the 2:1 resonance between Uranus and Neptune, the 7:1 resonance between Jupiter and Uranus, and with three-body resonances involving Jupiter, Saturn, and Uranus and Saturn, Uranus, and Neptune (see the section on analytic results, below). The variation of T_l with a_U is shown in figures 13 and 14. The few hundred million year length of most of the runs limited their ability

to place lower limits on T_l to about 100 Myr. More recently, we have extended some runs to 1 Gyr; the results of two runs are shown in Figure 15. The figure plots the phase space distance between two copies of the solar system, in which one copy of Uranus is displaced relative to the other by about 1 mm. There are two such calculations displayed, corresponding to two different fiducial values of a_U , 19.23, and 19.26. One is chaotic, the other is regular, or has T_l larger than about 0.5 Gyr. Note that an integration of less than 200 Myr would indicate that both systems were regular.

Murray & Holman also showed that many planar four-planet models were chaotic, indicating that inclination resonances were not required to produce chaotic motion in the outer planets. They demonstrated that a three-planet, nonplanar system without Neptune was often chaotic. However, a three-planet system with no Uranus or a three-planet planar problem with no Neptune was found to be completely regular, independent of the locations of the other planets (within moderate limits). One of the orbits, even in strongly chaotic systems, showed any sign of substantial changes in a , e , or i over the length of the integrations.

This result was extended by Ito & Tanikawa (2000) to the entire solar system, over several ~ 4 Gyr integrations, using a Wisdom-Holman integrator. The integrations confirm the finding that the solar system is chaotic. They also show that the orbits of the planets do not change appreciably over the age of the solar system; the full system of equations is not appreciably more unstable than Laskar's averaged system. An estimate of the diffusion time, similar to that given above, but using the results of Ito & Tanikawa (2000), predicts that Mercury will not suffer any catastrophic encounters for 10^3 or even 10^4 Gyr. We appear to be

safe for now.

5.2 Analytic Results

The numerical results described above suggest that the solar system is chaotic, with a Lyapunov time of about 5 Myr. This result is surprising, because the solar system is observed to be more than 4 Gyr old. Not so surprising is the result that the integrations are stable, in the sense that no close encounters, defined by one body entering the Hill sphere of another, are found. In fact, the results of Ito & Tanikawa (2000) indicate that no planet has suffered even moderate changes in semimajor axis, eccentricity, or inclination. Why does the solar system appear to be so chaotic and, if it is, why is it so resistant to catastrophe?

Recently, we found an analytic explanation of both results, short term chaos and long term stability, in the setting of the outer solar system (Murray and Holman 1999). We start with the observation that chaos results from the interaction of at least two resonances between motion in two or more different degrees of freedom. We have to find the resonances. For example, consider the “great inequality,” the near 5:2 resonance between Jupiter and Saturn. The orbital period of Jupiter is 4,332.588 days, whereas that of Saturn is 10,759.278 days, giving a ratio of 2.4833. The mutual perturbations of these planets produce large (relative to the mass ratio M_J/M_\odot or M_S/M_\odot) variations in λ when compared with the Keplerian value. The variation amounts to about 21 and 49 arcminutes in the longitude of Jupiter and Saturn, respectively, variations that were noted by astronomers in the eighteenth century. Mathematically, the resonance

is represented by the following terms in the disturbing function:

$$-\frac{\mathcal{G}M_S}{a_S} \sum_{k,q,p,r} \phi_{k,q,p,r}^{(2,5)} (a_S/a_J) e_S^k e_J^q i_S^p i_J^r \cos [2\lambda_J - 5\lambda_S + k\varpi_S + q\varpi_J + p\Omega_S + r\Omega_J]. \quad (14)$$

Recall that $2 - 5 + k + q + p + r = 0$, and that $p + r$ must be even. Furthermore, $(2n_J - 5n_S)/n_J \approx -1.33 \times 10^{-2}$; although this is small, it is much larger than the ratio of any of the secular frequencies with n_J ; for example, $\varpi_S/n_J \approx 2.6 \times 10^{-4}$. The small magnitude of the secular frequencies implies that including the secular frequencies will change the location (in semimajor axis) of the resonance only slightly. On the other hand, the rather large distance from exact resonance ($\sim 10^{-2}$ is large compared with the width of the resonance, as we show below) shows that the planets are not “in” resonance, i.e. none of the angles in the argument of the cosine in Equation (14) librate.

The last statement can be generalized: The only planets in the solar system involved in a two-body mean-motion resonance are Neptune and Pluto. These two bodies are in a 3:2 mean-motion resonance, as well as a number of secular resonances. The chaos seen in integrations of the giant planets, and in the solar system excluding Pluto, is not due to the interaction of two-body mean-motion resonances.

The fact that Jupiter and Saturn are not in resonance does not mean that the resonant terms given by (14) are negligible, however. They produce substantial variations in the semimajor axis (given by Equation 8 and similar terms) and in the longitudes of the two planets; it was the latter, which involve two powers of $(2n_J - 5n_S)/n_J \approx -1.33 \times 10^{-2}$ in the denominator, that is responsible for the 21 arcminute discrepancy seen in the longitude of Jupiter by the eighteenth century observers. These near-resonant terms also produce substantial variations in the

eccentricity and inclination of both planets.

For example, Saturn's gravity forces variations in $e_J \sin \varpi_J$ given by

$$e_J^{(2,5)} \sin \varpi_J \approx \frac{\mu_S}{(2 - 5n_S/n_J)} \frac{a_J}{a_S} \sum_{p>0} \phi_{k,p,q,r}^{(2,5)} e_S^k e_J^{p-1} i_J^q i_S^r \times \sin[2\lambda_J - 5\lambda_S + k\varpi_S + (p-1)\varpi_J + q\Omega_J + r\Omega_S], \quad (15)$$

where $\mu_S \equiv M_S/M$ is the mass ratio of Saturn to the Sun. The largest variation in e_J , corresponding to $k = 2$, $p - 1 = q = r = 0$ and $\phi_{2,1,0,0} \approx 9.6$, has an amplitude of about 3.5×10^{-4} . Numerical integrations yield 3.7×10^{-4} (Murray and Holman 1999). As shown in the following section, this variation in e_J plays a central role in producing chaos among the outer planets.

5.2.1 THREE-BODY RESONANCES

Although there are no two-body resonances between the giant planets, there are a number of resonances involving three bodies. Three-body resonances involve the longitudes of three planets; the combinations $3\lambda_J - 5\lambda_S - 7\lambda_U$ and $3\lambda_S - 5\lambda_U - 7\lambda_N$ are two examples. There are no terms containing such arguments in the disturbing function; they arise only at second order in the planetary masses. Physically, they arise as follows.

Consider Jupiter, Saturn, and Uranus. In the first approximation all three follow Keplerian orbits, so a , e , and i (as well as ϖ and Ω) are constant for all three bodies. At the next level of approximation, Saturn perturbs the orbit of Jupiter, and vice versa. This will, for example, cause tiny variations in e_J and e_S , as calculated in the previous section. The amplitude of the variation will be proportional to the mass of the perturbing planet.

Now consider the potential experienced by Uranus. To lowest order Uranus moves on a Keplerian orbit, so to first order in the masses it will see the potential

given by the disturbing function with the Keplerian values of e_J and so forth. At second order in the masses, several types of correction arise. One type is due to the fact that Uranus' orbit is not Keplerian. For example, Jupiter will force changes in a_U , e_U , and so forth, which have magnitude proportional to M_J and period given by $pn_J - qn_U$, where p and q are integers. The position vector \mathbf{r}_U will inherit oscillatory terms of this form. The potential experience by Uranus, due to Saturn, will in turn inherit terms proportional to M_J , with resonant arguments involving λ_J . This will lead to terms of the form $M_J M_S \cos[p\lambda_J - r\lambda_S - (s+q)\lambda_U]$. We refer to such terms as three-body resonances.

Three-body resonant terms arise in two other ways. We have already said that Saturn will produce variations in Jupiter's orbital elements of the form $M_S \cos[l\lambda_J - m\lambda_S]$. The potential experienced by Uranus, assumed to be on a Keplerian orbit, contains terms of the form $M_J e_J^l \cos[p\lambda_J - q\lambda_U + l\varpi_J]$. However, e_J is no longer constant; $e_J(t)$ contains terms of the form $M_S \cos[p\lambda_J - r\lambda_S]$. Once again, these will give rise to terms proportional to $M_J M_S$ containing resonant arguments involving all three mean longitudes.

Similarly, Jupiter will produce variations in Saturn's orbital elements, which will in turn affect the potential experienced by Uranus and give rise to terms proportional to the mass of both Jupiter and Saturn, and having resonant arguments involving all three planetary mean longitudes.

Murray and Holman (1997) gave analytic estimates of the strength, or width, and of the separation of such resonances. The width of a typical component resonance is

$$\frac{\Delta a}{a_U} = 8\sqrt{(6-p)\phi_{6-p,p,0,0}^{(7,1)}\phi_{2,1,0,0}^{(2,5)}\frac{\alpha}{3\epsilon}\mu_J\mu_S e_J^{5-p} e_U^p e_S^2} \approx 2 \times 10^{-6}, \quad (16)$$

where $\alpha = a_J/a_S \approx 0.55$ and $\epsilon = |2 - 5(n_S/n_J)|$ (n_S and n_J being the respective

mean-motions of Saturn and Jupiter). This yields $\Delta a \approx 8 \times 10^{-5}$ AU. The libration period associated with a resonance of this amplitude is

$$T_0 = T_U \left/ \sqrt{147(6-p)\phi_{6-p,p,0,0}^{(7,1)}\phi_{2,1,0,0}^{(2,5)}\frac{\alpha}{\epsilon}\mu_J\mu_S e_J^{5-p} e_U^p e_S^2} \right. \approx 10^7 \text{ years}, \quad (17)$$

where T_U is the orbital period of Uranus. This is essentially the Lyapunov time (Holman & Murray 1996, Murray & Holman 1997).

Murray & Holman (1999) estimate the time for Uranus to suffer a close encounter with Saturn. An ejection or collision would then follow in short order. The estimate assumes that there are no dynamical barriers to the random walk of e_U produced by the chaos. They find a time of order 10^{18} years, much longer than the current age of the Universe.

Figures 13 and 14 show the location of various two- and three-body resonances in the vicinity of Uranus. In figure 14 one can see individual three-body mean-motion resonances. The resonant argument of the resonance closest to the best estimate of the orbit of Uranus is seen to alternate between libration and rotation in figure (16)

5.2.2 CHAOS IN THE INNER SOLAR SYSTEM

The situation in the inner solar system is currently unclear. There have been a number of candidate resonances suggested, but no analytic calculations have been done. This is clearly an opportunity for an enterprising theorist.

Without a calculation in hand one cannot say what Lyapunov time one expects from overlap of secular resonances, or how to predict the time required for a planet's (Mercury in this case) orbit to change drastically. We can use estimates similar to that given in Equation (13), but they are on rather shaky ground because we do not know if the variations of e we see in the integrations

are primarily diffusive or if they are actually the result of quasiperiod forcing of Mercury's orbit by, e.g. Venus and Earth. There is some evidence for the latter, because both Laskar (1990, 1994), Laskar et al (1992), Sussman & Wisdom (1992), and Ito & Tanikawa (2000) find strong correlations between the motion of all three planets. If the variations in the eccentricity of Mercury are primarily due to quasiperiodic forcing, then Mercury's lifetime could be much longer than our estimate.

From the numerical results of Laskar (1994) and Ito & Tanikawa (2000) we gave a rough estimate of 10^{13} years for the lifetime of Mercury. Murray & Holman (1999) found 10^{18} years for the lifetime of Uranus. In units of orbital periods these lifetimes are 4×10^{13} and 10^{16} , a ratio of about 250, yet the Lyapunov times of the two systems are within a factor of about two. Without an analytic theory for the chaos in the inner solar system it is difficult to assess the significance of this discrepancy.

We have noted that the resonance σ_1 identified by Laskar does not overlap with any other secular resonance that has so far been identified. This suggests that it is not the source of the chaotic motion seen in various integrations. Rather, it appears that the transitions between libration and rotation are the result of chaotic forcing by other planets. This may be checked by integrations of the solar system excluding Mercury, in which Uranus is moved to a location outside the chaotic three-body mean-motion resonances. If the resulting system is still chaotic, then the resonance corresponding to σ_1 does not play an essential role in producing the chaos seen in the integrations.

6 SUMMARY AND SUGGESTIONS FOR FURTHER WORK

The solar system is unstable, although on times much longer than the Lyapunov times. Our main task is to identify the resonances that overlap and induce chaos and to predict the ejection time as a function of the Lyapunov time (which is relatively easy to calculate). For example, in the region of overlapping first-order mean-motion resonances the ejection time is proportional to the Lyapunov time to the 1.75 power. A similar power law relation, with a different exponent, holds for high-order mean-motion resonances, where the various subresonances overlap. As yet, we have no such relation for secondary resonances, where the libration frequency is a multiple of the apsidal motion. Surprisingly, the relation with the exponent of 1.75 holds approximately throughout the solar system, although the spread in ejection times for 90% of the trajectories is a factor of 10 on either side of the prediction, (see figure 17). The exceptions occur at high-order mean-motion resonances or at overlapping secular resonances. The “diffusion” among the subresonances inside the same mean-motion resonance is much slower than the diffusion between overlapping first-order mean-motion resonances. The relevant model for chaos in the solar system is the overlap of two resonances; in the Hamiltonian formulation this resembles a pendulum driven at resonance. This induces a random walk (diffusion) in the eccentricity that can result in a close encounter with the perturber and a radical change in the orbit. We do not believe that a web of resonances (the Arnold Web) is relevant for chaos in the solar system, as interesting as that formulation is mathematically, and we no longer believe that instability is caused by a secular drift in the semimajor axes.

Three-body resonances have been identified as the source of chaos for the outer planets. Because these resonances are proportional to the product of the mass

ratios of the two planets to the Sun, the time scale is quite long, on the order of 10^9 times the age of the solar system.

The identification of the overlapping secular resonances in the inner solar system (the terrestrial planets) is not firm, but an extrapolation of the numerical integration indicates that Mercury will be in trouble in 10^{13} years (well after the Sun becomes a red giant and engulfs Mercury).

The work we have reviewed here could be termed ‘weak chaos’. We picked up the story after the violent encounters associated with the formation of the Solar System were over. The trajectories we studied could be treated by the well-developed methods of modern non-linear dynamics and celestial mechanics. The discovery of extra-solar planets draws our attention to the era of formation when the planetary bodies were less well-behaved; when close encounters, collisions, mergers, and ejections were the norm. That was the era of ‘strong chaos’. Exploring this should provide the palette of stable configurations.

Literature Cited

- Aksnes K. 1988. In *Long-term Dynamical Behavior of Natural and Artificial N-Body Systems*, ed. A. E. Roy, pp. 125–39. New York: Klumer Academic Pub.
- Applegate J, Douglas MR, Gursel Y, Sussman GJ, Wisdom J. 1986. *Astron. J.* 92:176–94
- Arnold VI. 1978. *Mathematical Methods of Classical Mechanics*. New York: Springer-Verlag
- Brouwer D, Clemence GM. 1961. *Methods of Celestial Mechanics*. New York: Academic
- Chirikov BV. 1979. *Phys. Rep.* 52:265–376
- Duncan M, Levison H. 1997. *Science* 276:1670–72
- Duncan MJ, Levison HF, Budd SM. 1995. *Astron. J.* 110:3073–81
- Duncan M, Quinn T. 1993. *Annu. Rev. Astron. Astrophys.* 31:265–95
- Duncan M, Quinn T, Tremaine S. 1989. *Icarus* 82:402–18
- Duncan M, Quinn T, Tremaine S. 1988. *Astrophys. J.* 328:L69–73

- Edgeworth K. 1943. *J. Brit. Astron. Soc.* 53:181-88
- Edgeworth K. 1949. *Mon. Not. R. Astron. Soc.* 109:600-9
- Evans NW, Tabachnik S. 1999. *Nature* 399:41-43
- Everhart E. 1973. *Astron. J.* 78:329-37
- Farinella P, Froeschle Ch, Froeschle C, Gonczi R, Hahn G, Morbidelli A, Valsecchi G. 1994. *Nature* 371: 315-317
- Farinella P, Davis DR, Stern SA. 2000. See Mannings et al 2000, p. 1255-1282
- Fernandez J. 1980 *Mon. Roy. Astron. Soc.* 192:481-491
- Ferraz-Mello S., Klafke J. 1991. In *Predicibility, Stability and Chaos in N-Body Dynamical Systems*, ed. A. E. Roy, p. 177. New York: Plenum Press.
- Franklin F, Lecar M, Soper P. 1989. *Icarus* 79:223-27
- Franklin F, Lecar M, Wiesel W. 1984. In *Planetary Rings*, ed. R Greenberg, A Brahic, pp. 562-88. Tucson: Univ. Ariz.
- Franklin F. 1994. *Astron. J.* 107:1890-99
- Franklin F. 1996. *Astron. J.* 112:1247-53
- Franklin F, Lecar M. 2000. *Meteor. and Planet. Sci.* 35:331-40
- Gallardo T, Ferraz-Mello S. 1998. *Planetary and Space Science* 46:945-65
- Giffen R. 1973. *Astron. Astrophys.* 23:387-403
- Gladman BJ, Duncan MJ. 1990. *Astron. J.* 100:1680-93
- Gladman B, Migliorini F, Morbidelli A, Zappala P, Michel P, Cellino A, Froeschle Ch, Levison H, Bailey M, Duncan M. 1997. *Science* 277:197-201
- Grazier K, Newman W, Varadi F, Kaula W, Hyman J. 1999a. *Icarus* 140:341-52
- Grazier K, Newman W, Varadi F, Kaula W, Hyman J. 1999b. *Icarus* 140:353-68
- Hénon M. 1983. In *Chaotic Behavior of Deterministic Systems*, ed. G Iooss, RHG Helleman, R Stora, pp. 53-170. Amsterdam, North-Holland.
- Henrard J, Lemaître A. 1986. *Cel. Mech. Dyn. Ast.* 39:213-38
- Henrard J, Watanabe N, Moons M. 1995. *Icarus* 115:336-46
- Holman M. 1995. In *Proc. 27th Symp. Celest. Mech.*, January 10-11, ed. H Kinoshita, H Nakai, National Astronomical Observatory, Mitaka, Japan.
- Holman M. 1997. *Nature* 387:785-88

- Holman M, Murray N. 1996. *Astron. J.* 112:1278–93
- Holman M, Wisdom J. 1993. *Astron. J.* 105:1987–99
- Ip W-H, Fernandez J. 1997. *Astron. Astrophys.* 324:778–84
- Ito T, Tanikawa K. 2000. In *Proc. 32nd Symp. Celest. Mech.*, ed. H Arakida, Y Masaki, H Umehara, pp. 47–96. Hayama, Japan: Graduate Univ. Advanced Stud.
- Jewitt D, Luu J. 2000. See Mannings et al 2000, pp. 1201–1230
- Jewitt D, Luu J. 1993. *Nature* 362:730–732 See Mannings et al 2000, pp. 1201–1230
- Kirkwood D. 1867. *Meteoric Astronomy: a treatise on shooting-stars, fireballs, and aerolites*, Philadelphia: Lippincott
- Knežević Z, Milani A, Farinella P, Froeschle Ch, Froeschle Cl. 1991. *Icarus* 93:316–30
- Kuiper G. 1951. In *Astrophysics*, ed. J Hynek, pp 357–424. New York: McGraw-Hill
- Laskar J. 1985. *Astron. Astrophys.* 144:133–46
- Laskar J. 1989. *Nature* 338:237–38
- Laskar J. 1990. *Icarus* 88:266–91
- Laskar J. 1992. In *Chaos, Resonance and Collective Dynamical Phenomena in the Solar System*, ed. S Ferraz-Mello, pp 1–16. Dordrecht, The Netherlands: Kluwer
- Laskar J. 1993. *Cel. Mech. Dyn. Ast.* 56:191–6
- Laskar J. 1994. *Astron. Astrophys.* 287:L9–12
- Laskar J, Quinn T, Tremaine S. 1992. *Icarus* 95:148–52
- Lecar M. 1996. In *Chaos in Gravitational N-Body Systems*, ed. JC Muzzio, S Ferraz-Mello, J Henrard, pp. 163–66. Dordrecht, The Netherlands: Kluwer
- Lecar M, Franklin F. 1973. *Icarus* 20:422–36
- Lecar M, Franklin F, Murison M. 1992. *Astron. J.* 104:1230–36
- Lecar M, Franklin F. 1997. *Icarus* 129:134–46
- Lemaitre A, Henrard J. 1990. *Icarus* 83:391–409
- Le Verrier U-J. 1855. *Ann. Observ. Imp. Paris* 1:1–258
- Levison H, Duncan M. 1993. *Astrophys. J.* 406:L35–38
- Levison H, Duncan M. 1997. *Icarus* 127:13–32
- Lichtenberg AJ, Lieberman MA. 1992. *Regular and Chaotic Dynamics*. New York: Springer-Verlag. 2nd ed.

- Liou, JC, Malhotra, R. 1997. *Science* 275:375–77
- Luu J, Marsden B, Jewitt D, Trujillo C, Hergenrother C, Chen J, Offutt W. 1997. *Nature* 387:573–576
- Malhotra R, Duncan M, Levison H. 2000. See Mannings et al 2000, pp. 1231–1254
- Malhotra R. 1996. *Astron. J.* 111:504–16
- Malhotra R, Williams J. 1997. In *Pluto and Charon*, eds. D J Tholen & S A Stern, pp. 127–57. Tucson: Univ. Arizona Press
- Mannings V, Boss A, Russell S, eds. 2000. *Protostars & Planets IV*. Tucson: Univ. Ariz. Press
- Mikkola F, Innanen K. 1995. *Mon. Not. R. Astron. Soc.* [**AU: Please spell out Mon. Not., Monthly Notices **] 277:497–501
- Mikkola F, Innanen K. 1999. *Cel. Mech. Dyn. Ast.* 74:59–67
- Milani A, Nobili AM, Fox K, Carpino M. 1986. *Nature* 319:386–88
- Moons M, Morbidelli A. 1995. *Icarus* 114:33–50
- Moons M. 1997. *Cel. Mech. and Dyn. Astron.* 65:175–204
- Moons M, Morbidelli A, Migliorini F. 1998. *Icarus* 135:458–68
- Morbidelli A. 1996. *Astron. J.* 111:2453–61
- Morbidelli A. 1997. *Icarus* 127:1–12
- Morbidelli A, Moons M. 1993. *Icarus* 103:99–108
- Morbidelli A, Thomas F, Moons M. 1995. *Icarus* 118:322–40
- Moser J. 1973. *Stable and Random Motions in Dynamical Systems*, Princeton, NJ: Princeton Univ. Press
- Murray CD, Dermott SF. 1999. *Solar System Dynamics*, Cambridge: Cambridge Univ. Press
- Murray CD, Harper D. 1993. *Expansion of the planetary disturbing function to eighth order in the individual orbital elements*, QMW Maths Notes, Sch. Math. Sci., London
- Murray N, Holman M. 1997. *Astron. J.* 114:1246–59
- Murray N, Holman M. 1999. *Science* 283:1877–81
- Murray N, Holman M, Potter M. 1998. *Astron. J.* 116:2583–89
- Nesvorný D, Ferraz-Mello S. 1997. *Icarus* 130:247–58
- Nesvorný D, Morbidelli A. 1998. *Astron. J.* 116:3029–37
- Nobili AM, Milani A, Carpino M. 1989. *Astron. Astrophys.* 210:313–36

- Oort J. 1950. *Bull. Astron. Inst. Netherl.* 11:91-110
- Ott E. 1993. *Chaos in Dynamical Systems*, Cambridge: Cambridge Univ. Press
- Peirce B. 1849. *Astron. J.* 1:1-8
- Peterson I. 1993. *Newton's Clock, Chaos in the Solar System*. New York: Freeman
- Poincaré H. 1993. *Methodes nouvelles de la mecanique celeste/New methods of celestial mechanics*, ed. D Goroff. Woodbury, NY: American Institute of Physics.
- Quinn T, Tremaine S, Duncan M. 1990. *Astrophys. J.* 355:667-79
- Reichl LE. 1992. *The Transition to Chaos*. New York: Springer-Verlag
- Sagdeev RZ, Usikov DA, Zaslavsky GM. 1988. *Nonlinear Physics, From the Pendulum to Turbulence and Chaos*. Chur, Switzerland: Harwood
- Soper P, Franklin F, Lecar M. 1990. *Icarus* 87:265-84
- Sussman GJ, Wisdom J. 1988. *Science* 241:433-37
- Sussman GJ, Wisdom J. 1992. *Science* 257:56-62
- Šidlichovský M. 1990. *Cel. Mech. Dyn. Ast.* 49:177-96
- Torbett M. 1989. *Astron. J.* 98:1477-81
- Torbett M, Smoluchowski R. 1990. *Nature* 345:49-51
- Weibel W, Kaula W, Newman W. 1990. *Icarus* 83:382-90
- Williams, JG. 1969. PhD thesis Univ. Calif. Los Angeles.
- Wisdom J. 1980. *Astron. J.* 85:1122-33
- Wisdom J. 1982. *Astron. J.* 87:577-93
- Wisdom J. 1983. *Icarus* 56:51-74
- Wisdom J. 1985. *Icarus* 63:272-89
- Wisdom J, Holman M. 1991. *Astron. J.* 102:1528-38
- Yu Q, Tremaine S. 1999. *Astron. J.* 118:1873-81

Figure 1: (a) A case of (temporary) secular resonance within the 3:1 mean-motion resonance. Dark solid line here and elsewhere marks the motion of Jupiter’s apse, ϖ_J , showing the effect of the longer term ν_5 and shorter ν_6 variation. Crosses correspond to a body with $a_0 = 0.481$ [$a_{Jup} = 1.0$] and $e_0 = 0.05$. (b) Eccentricity, e , surges that develop from the case of secular resonance shown in (a). e ’s > 0.32 cause a crossing of Mars’ orbit. Note that the condition $\varpi_A > \varpi_J$ corresponds to an increase in e .

Figure 2: Secular resonances within the 5:2 resonance, after Moons & Morbidelli (1995). Two broad lines mark the limits (“separatrices”) of 5:2, and the central line periodic solutions of the restricted three-body problem. Lower (upper) thin solid lines are the loci of the ν_6 (ν_5) secular terms and the dashed lines, their approximate limits. Central hatched region contains nonchaotic orbits (cf figure 4d,e). Note that orbits with $e < 0.2$ have a vanishing chance of escaping the effects of both ν_5 and ν_6 and hence are especially chaotic.

Figure 3: Distribution of 58,000 asteroids with reliable orbits from the most current files of the Minor Planet Center. Principal mean-motion resonances are indicated. The gap/boundary near $a = 2.08$ AU results from the strong perturbations on e’s and i’s due to the ν_6 and ν_{16} secular resonances.

Figure 4: A typical example of a regular orbit, $a_0 = 0.481$, $e_0 = 0.40$, libration amplitude 8° degrees, lying with the 3:1 resonance. (a) shows that it is unaffected by secular resonance; (b) plots the separation in longitude with time for two bodies with the above elements that are identical except for an initial longitude difference of 10^{-6}° . This body's essentially zero slope implies a very long Lyapunov time and consequently an orbit that shows no sign of being chaotic. (c) shows that its eccentricity variations guarantee frequent crossing of Mars' orbit, which requires only $e > 0.35$.

Figure 5: Examples of chaotic and regular behavior at the 5:2 mean-motion resonance. The large amplitude oscillations of $\varpi_A - \varpi_J$ in (a) lead to a chaotic orbit with a Lyapunov time, given by the slope in (b) of $\log T_l = 3.01$ in P_J . Its eccentricity regularly exceeds 0.5. The smaller oscillations shown in (c) corresponds to a far more regular orbit with $\log T_l > 5.6$. Despite formally lying in the ν_5 secular resonance, such orbits show no signs of escape or e increase beyond 0.35 in integrations of a planar model extending to 2 billion years.

Figure 6: Survival and escape times at resonances in the outer asteroid belt after Murray & Holman (1997). Open and filled symbols correspond to predicted and numerical estimates, arrows to lower limits.

Figure 7: Locations of secondary resonances, defined by the ratio of apsidal to libration periods, lying within the 2:1 mean-motion resonance for a semimajor axis $a_0 = 0.630$ ($a_J = 1.0$). Vertical scale measures degree of chaos by plotting the Lyapunov time, T_l , in Jovian orbital periods. As the eccentricities of Jupiter and Saturn are artificially reduced in (b) and (c), the influence of secondary resonances falls and orbits become more regular. Note in the insert in (a) that a few regular orbits do exist exactly at the 3/2 secondary resonance even when the eccentricities of the two planets are not lowered. As indicated, they are also found at 7/1, 11/1, and 12/1. Proper eccentricities of hypothetical bodies are about 0.03 larger than the plotted initial values. Libration amplitudes range from 2° at $e_0 = 0.25$ to 60° at $e_0 = 0.02$. All orbits plotted at $\log T_l > 5$ (usually 5.5) have T_l 's too long to be safely determined from unrenormalized integrations of at least 200,000 P_J and hence can be regarded as regular.

Figure 8: A sample of regular and chaotic orbits at the 3:2 mean-motion resonance. In (a) Jupiter and Saturn move in a planar approximation to their present orbits, but in (b) their eccentricities only have been increased by a factor of two so that their average values become 0.088 and 0.094. These higher e 's (though only Jupiter's is important) have the effect of broadening and deepening the 2/1 secondary resonance, as is shown in (c), but the enhancement is far less than at the 2:1 mean-motion resonance.

Figure 9: Dynamical lifetime throughout the outer solar system. At each semi-major axis bin, six test particles were started at different initial longitudes. The solid curve marks the trace of the minimum time survived as a function of semi-major axis. The points mark the survival times of the other particles, indicating the spread in dynamical lifetime. For reference, the semimajor axes of Jupiter, Saturn, Uranus, and Neptune are 5.2, 9.5, 19.2, and 30.1 AU, respectively.

Figure 10: The vertical axis shows the double logarithm of the final phase space separation of initial nearby test particles. This is proportional to the estimated Lyapunov time. The conversion to Lyapunov time is marked inside the left vertical axis. Figure from Mikkola & Innanen (1995).

Figure 11: Similar to figure 9, this shows the survival time versus semimajor axis in the inner planet region. Here the vertical axis is linear rather than logarithmic. The positions of the terrestrial planets are marked for reference. Figure from Evans & Tabachnik (1999).

Figure 12: The dynamical lifetime in the Kuiper belt as a function of semimajor axis and eccentricity, from Duncan et al (1995). The lifetime is color-coded. Long-lived regions can be seen at the locations of mean motion resonances with Neptune.

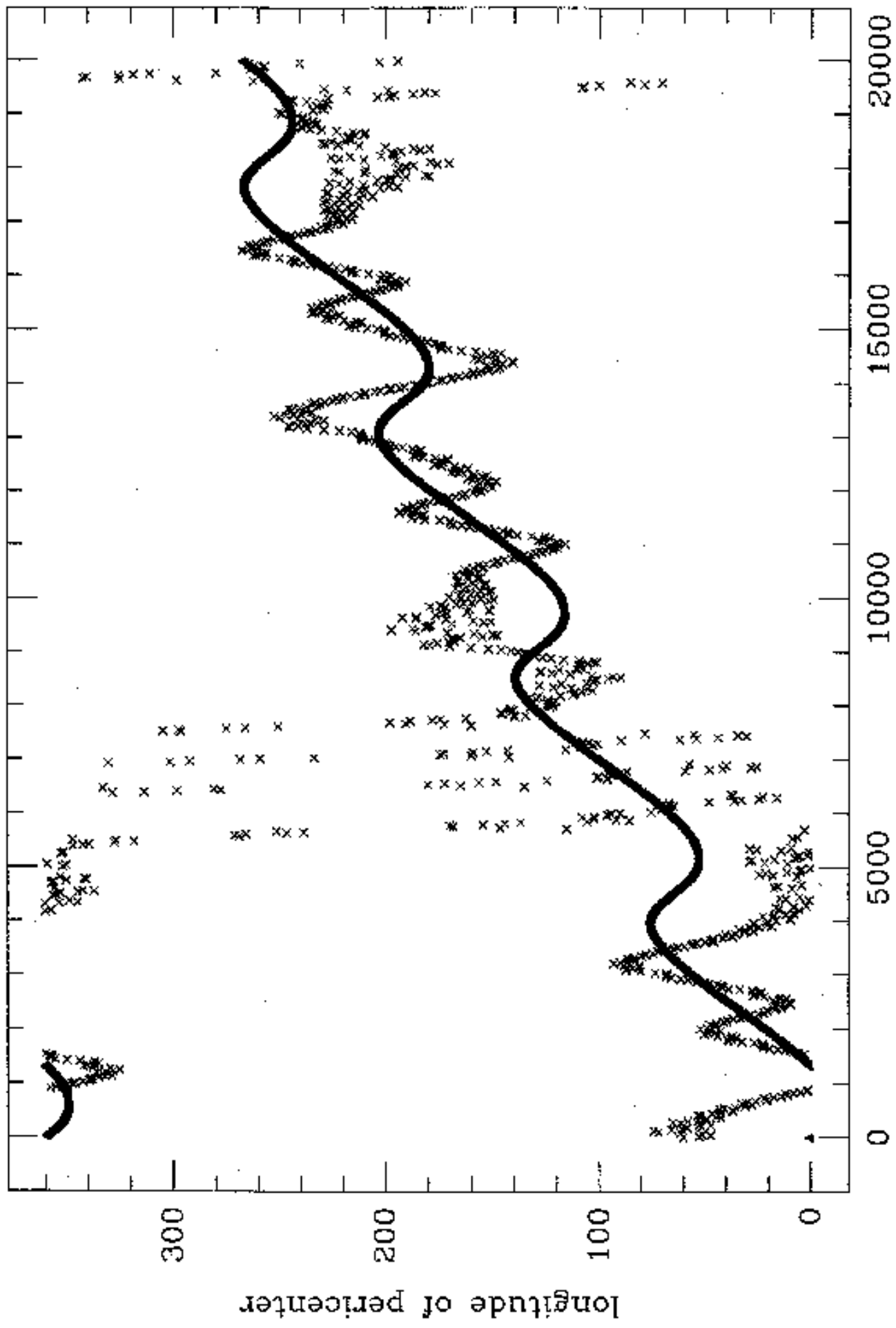
Figure 13: The Lyapunov time T_l of the system consisting of the four giant outer planets Jupiter, Saturn, Uranus, and Neptune. The semimajor axis of Uranus is varied around the best estimate of $a_U = 19.2189$, keeping all other elements fixed. One can see the 2:1 resonance with Neptune from 19 to 19.1, the 7:1 resonance with Jupiter at 19.18, and numerous three-body resonances at 19.22, 19.26, 19.3, and 19.34.

Figure 14: An enlarged version of figure 13 around 19.22 showing individual mean-motion resonances.

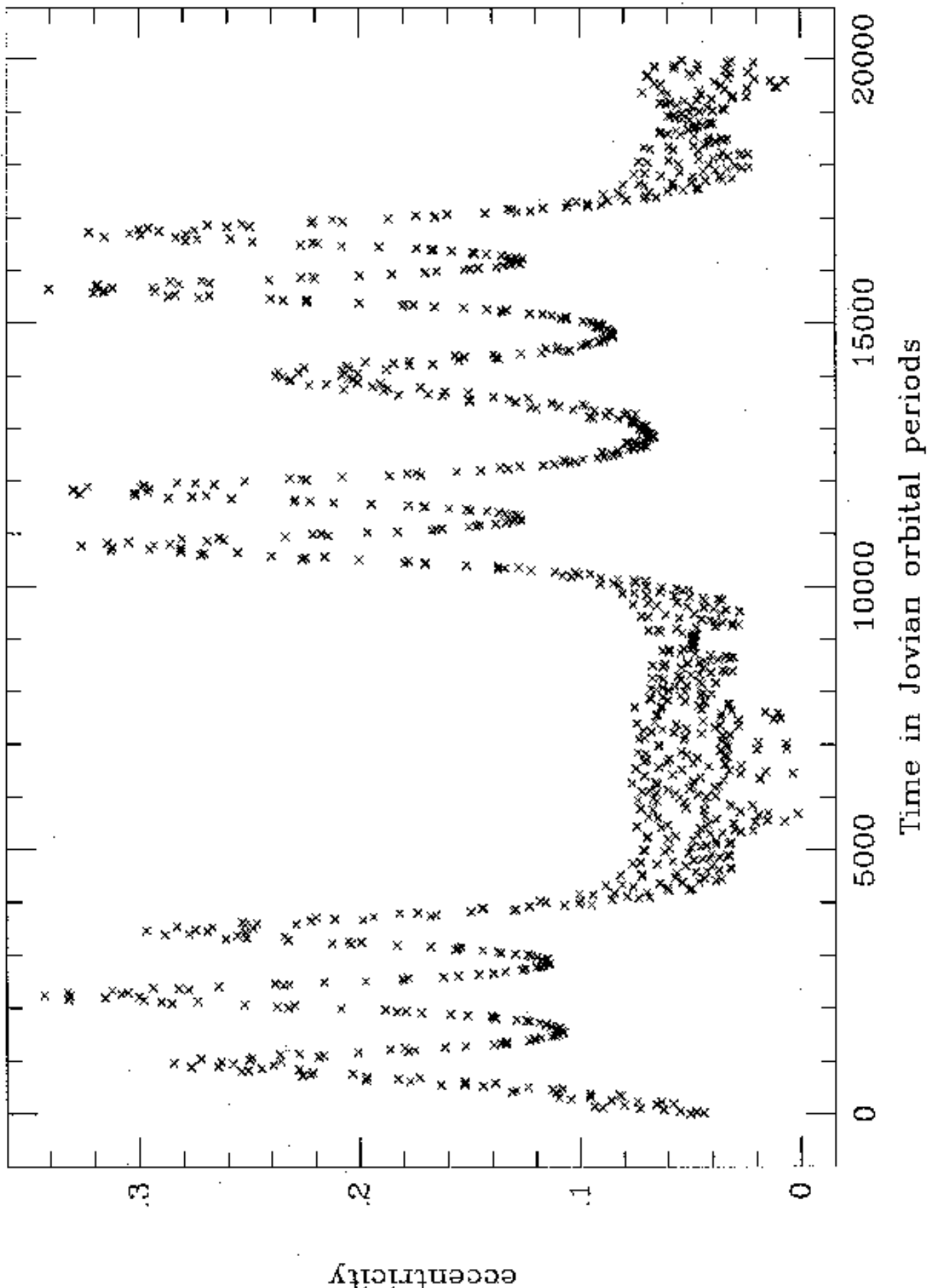
Figure 15: The phase space distance $\ln[d(t)]$ between two slightly ($1mm$) displaced copies of the four giant planets. Two integrations are shown, one with $a_U = 19.23$ and one with $a = 19.26$. Both appear to follow power laws for the first 200 Myr, but one eventually shows rapid separation and hence is chaotic. The other appears to be regular.

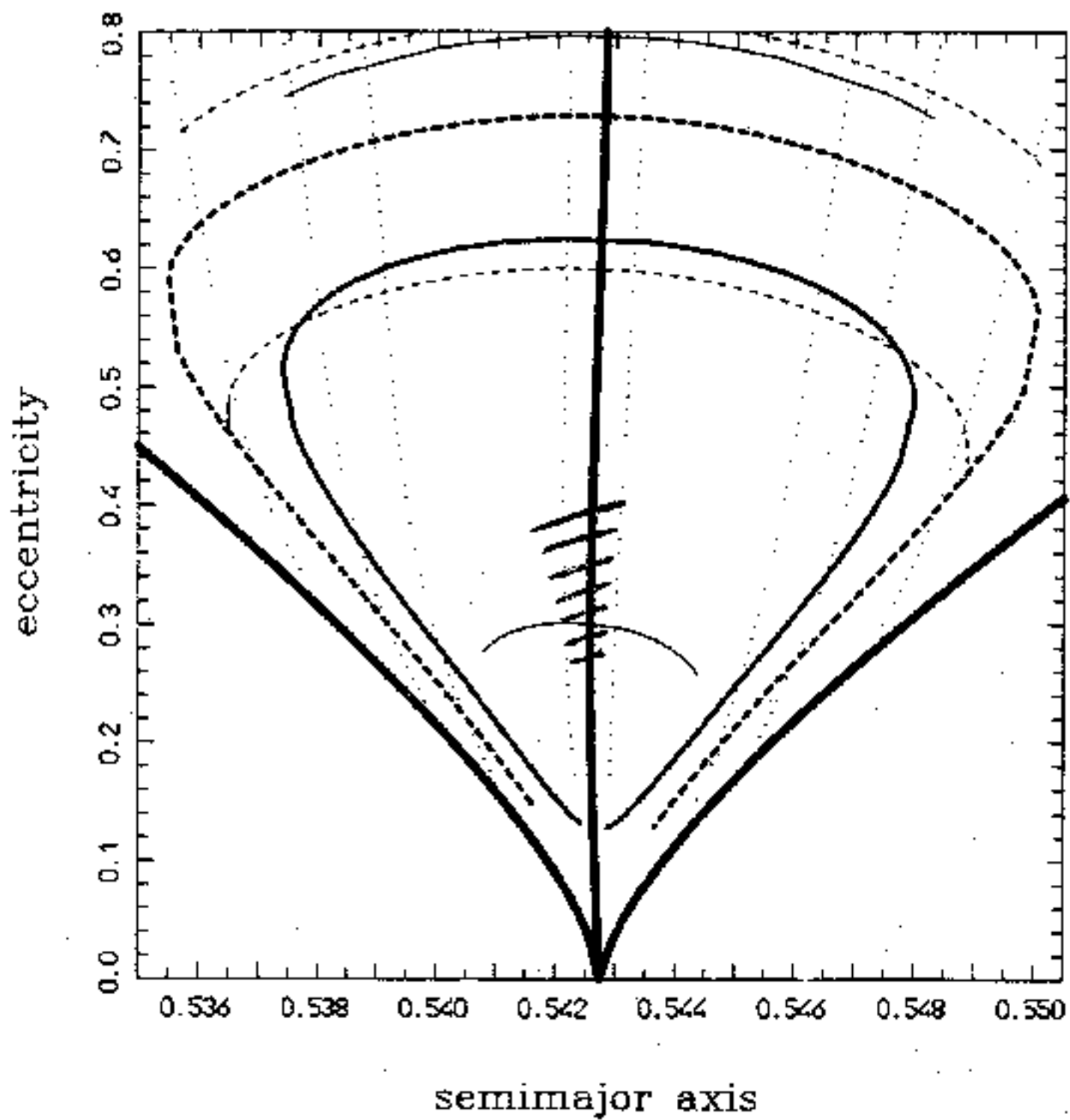
Figure 16: The resonant argument $3\lambda_J - 5\lambda_S - 7\lambda_U + 3g_5t + 6g_6t$. The libration period is about 20 Myr. One can see transitions from libration to rotation and back, eventually followed by a long period of rotation.

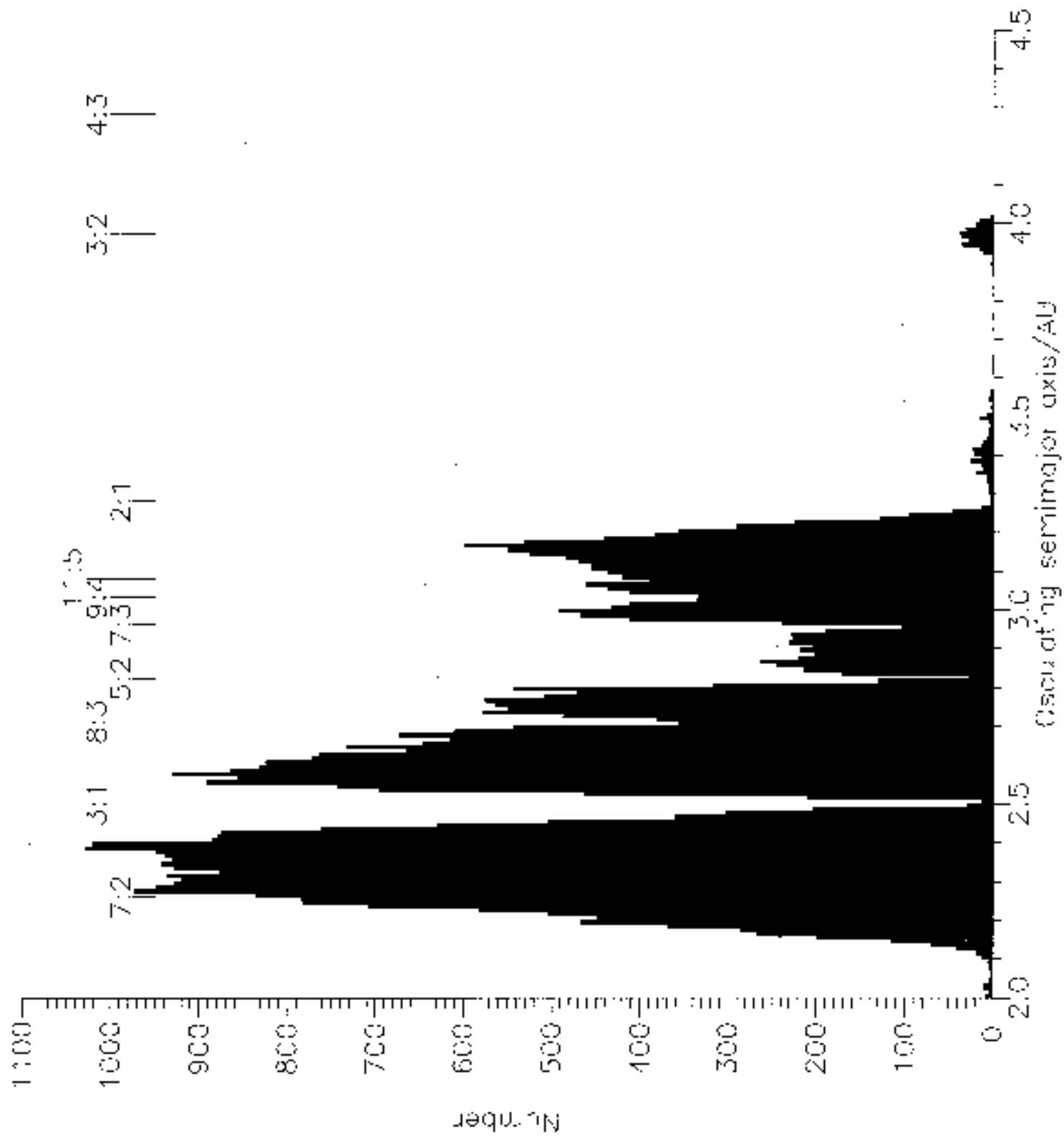
Figure 17: The ejection time, T_c , versus the Lyapunov time, T_l , in units of the period of the test particle. About 90% of the points fall within a factor of 10 of the relation, $T_c \sim T_l^{1.75}$.

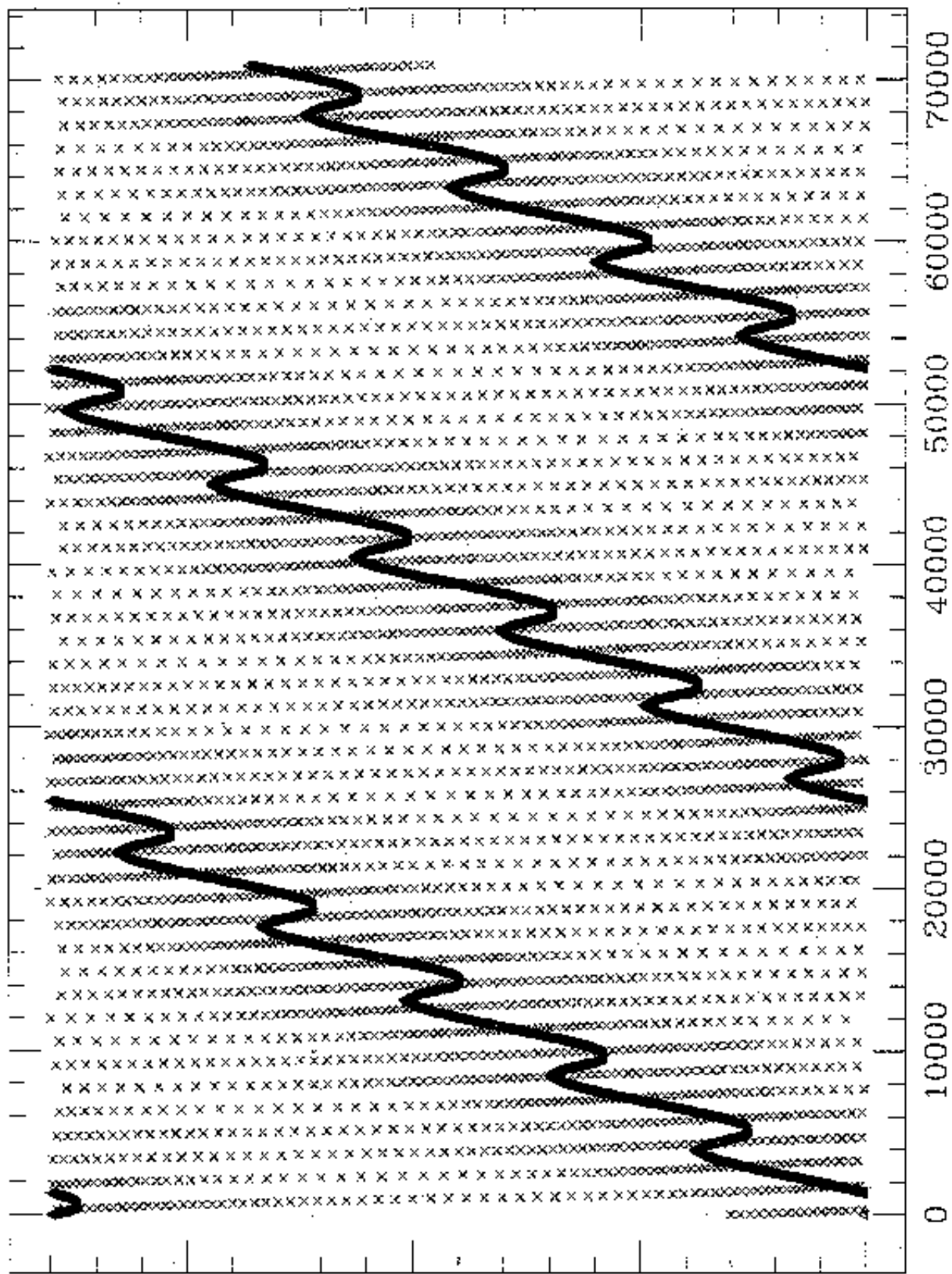


Time in Jovian orbital periods

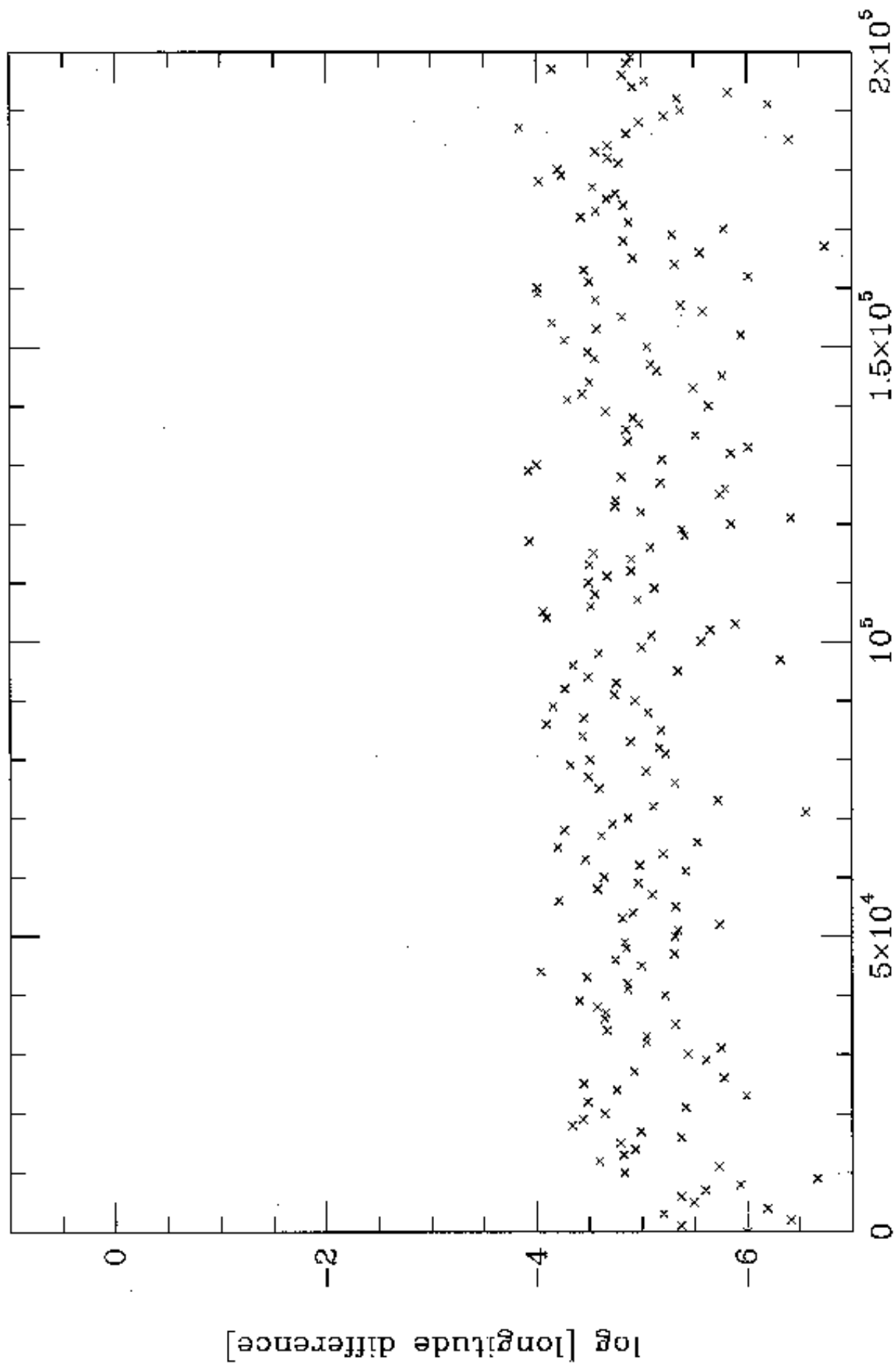




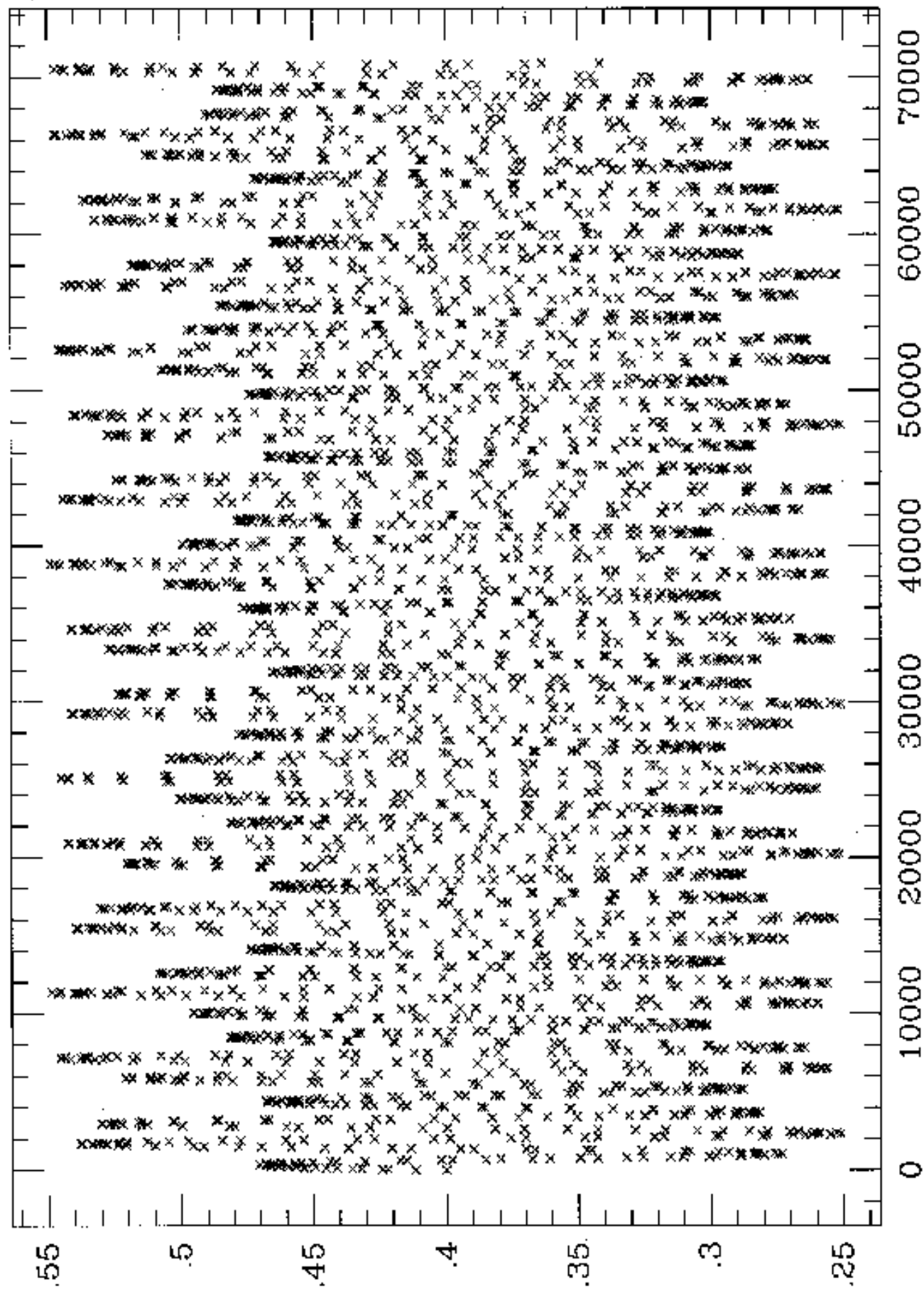




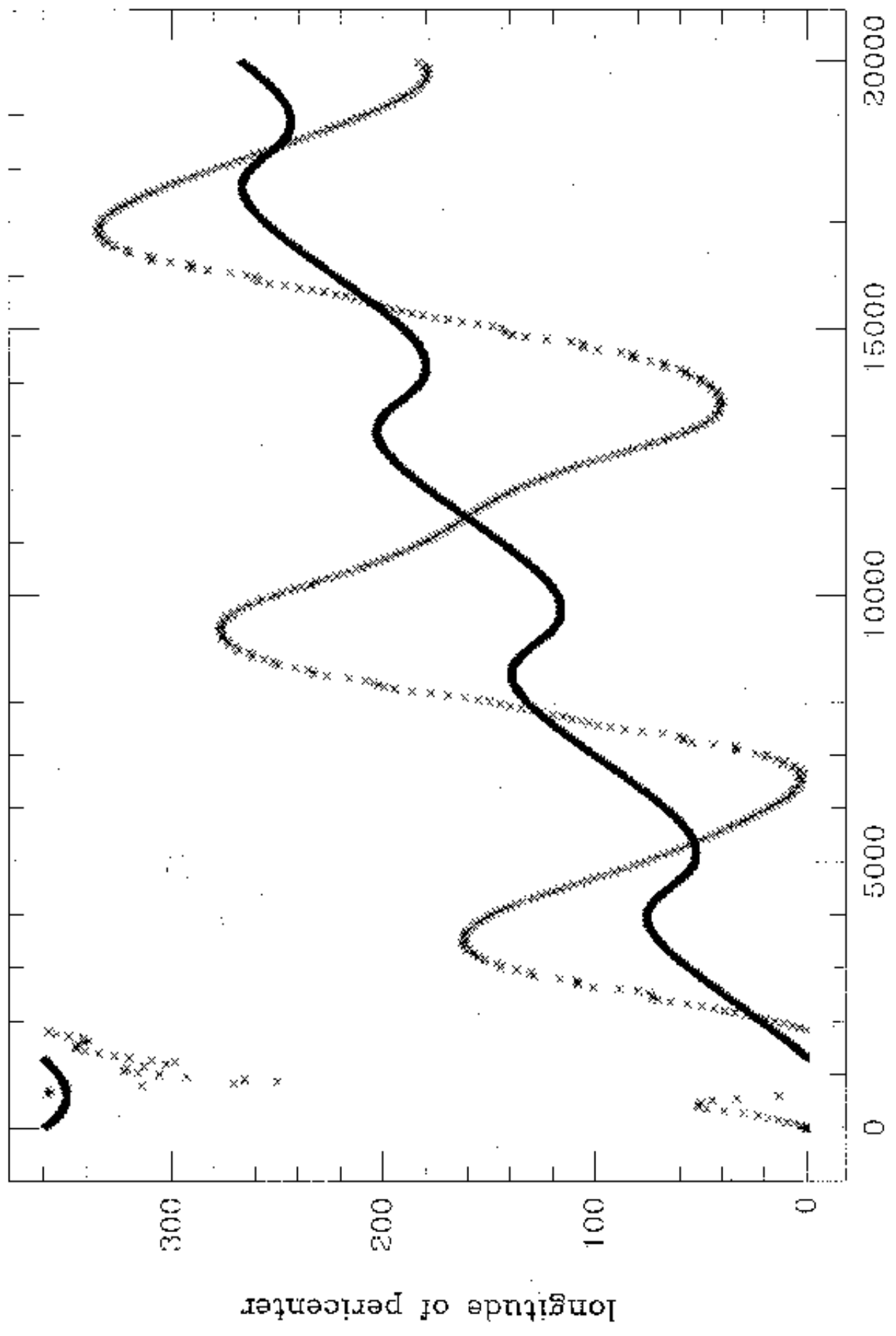
Time in Jovian orbital periods



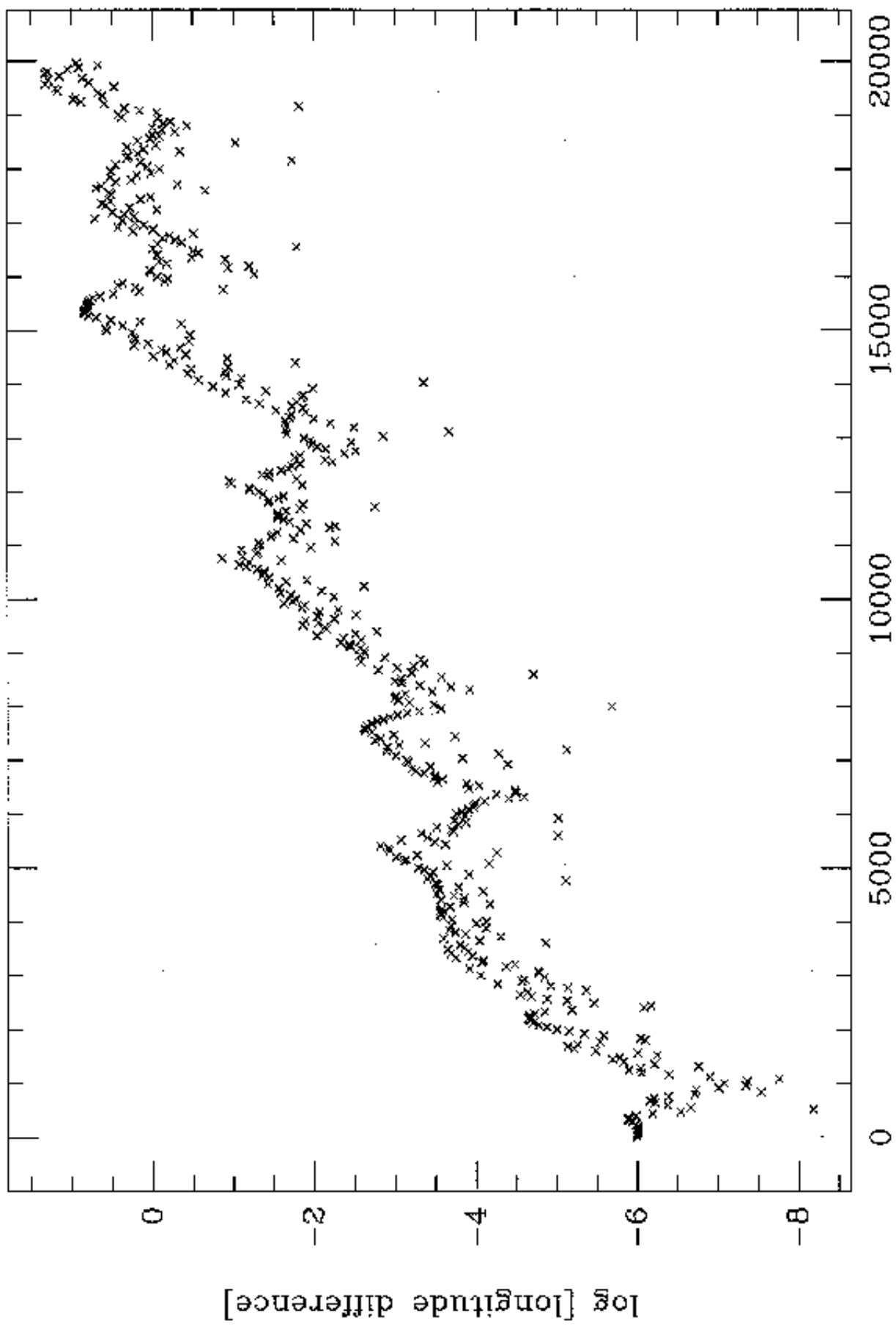
Time in Jovian orbital periods



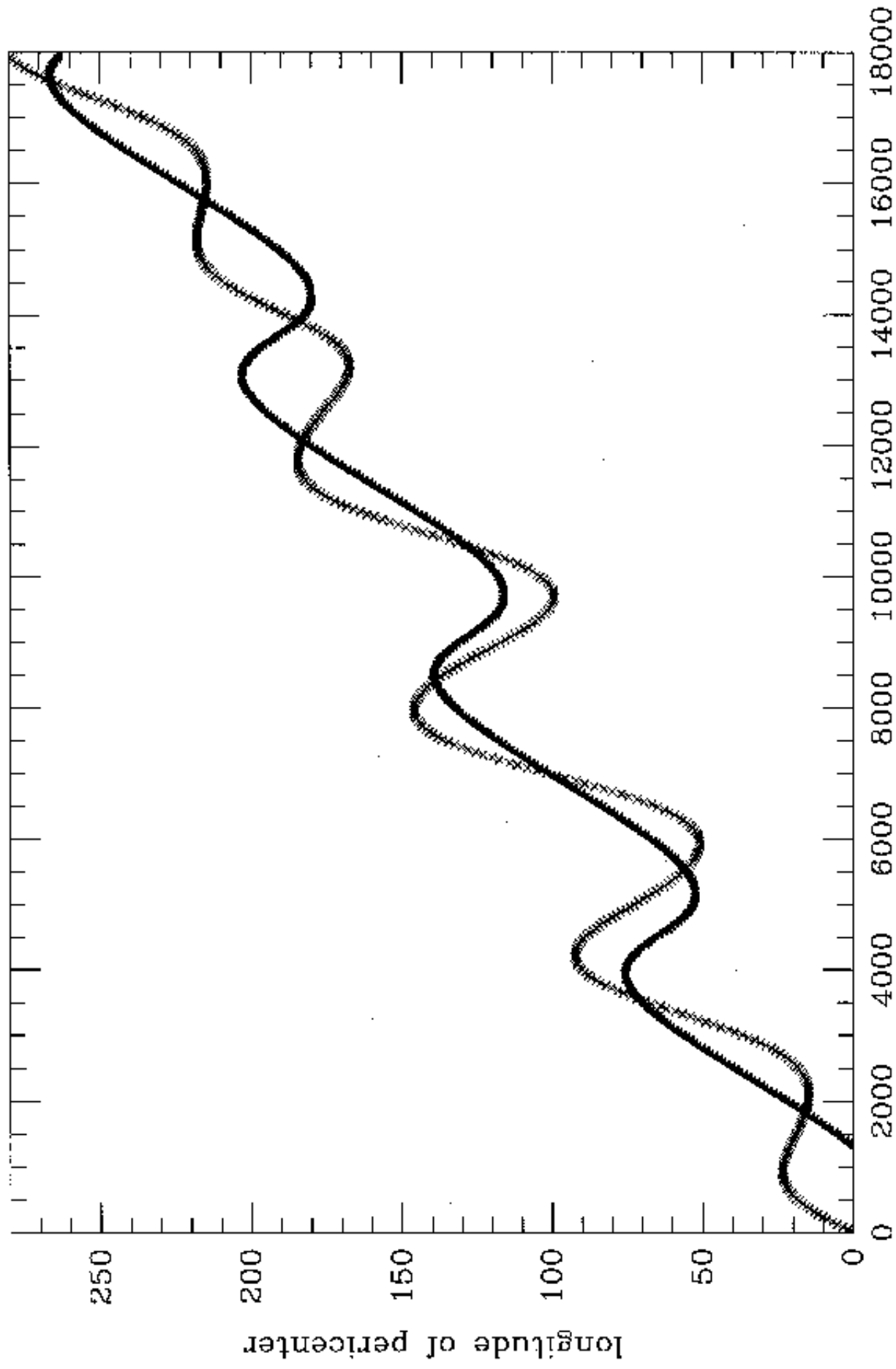
Time in Jovian orbital periods



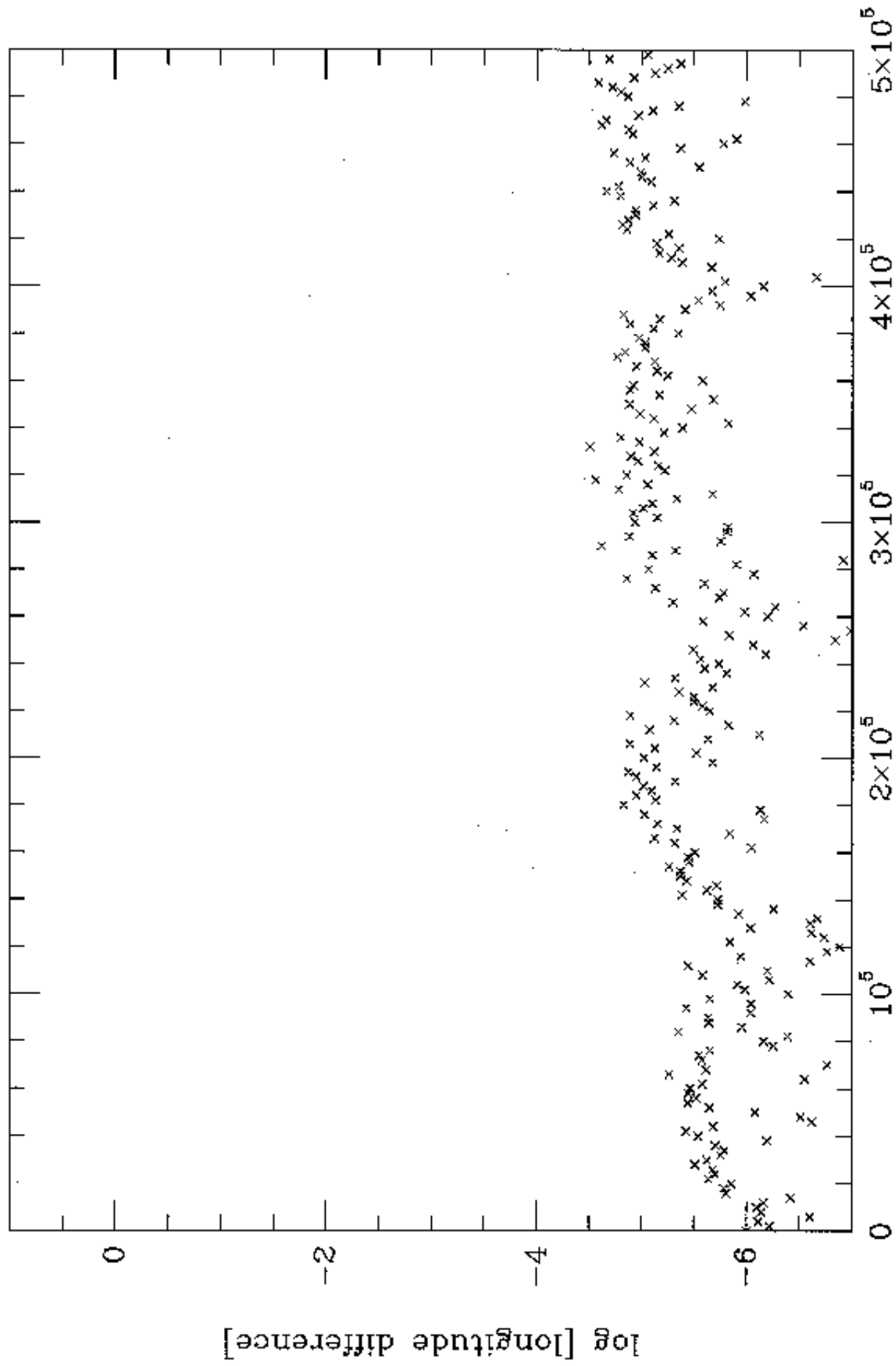
Time in Jovian orbital periods



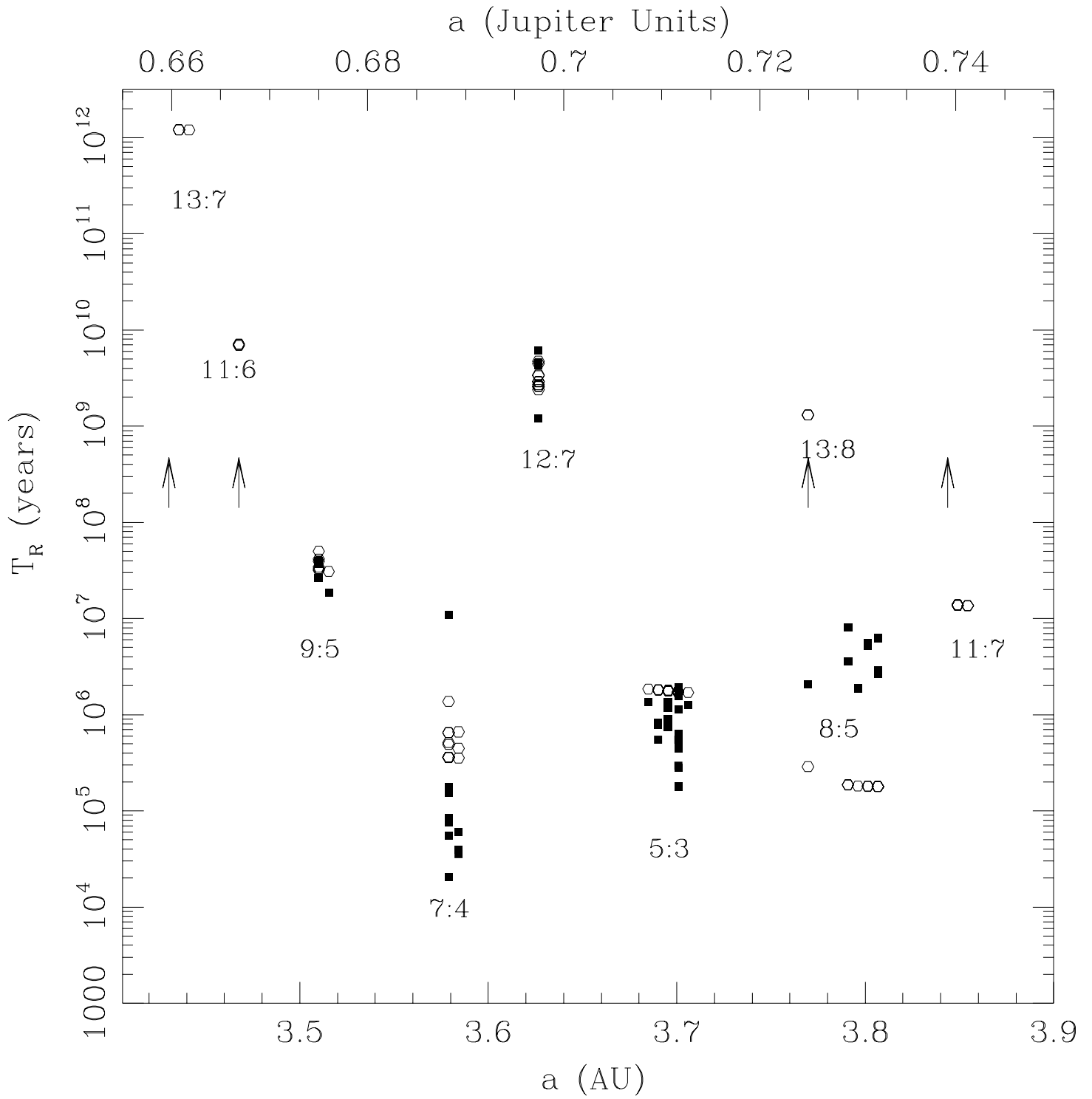
Time in Jovian orbital periods

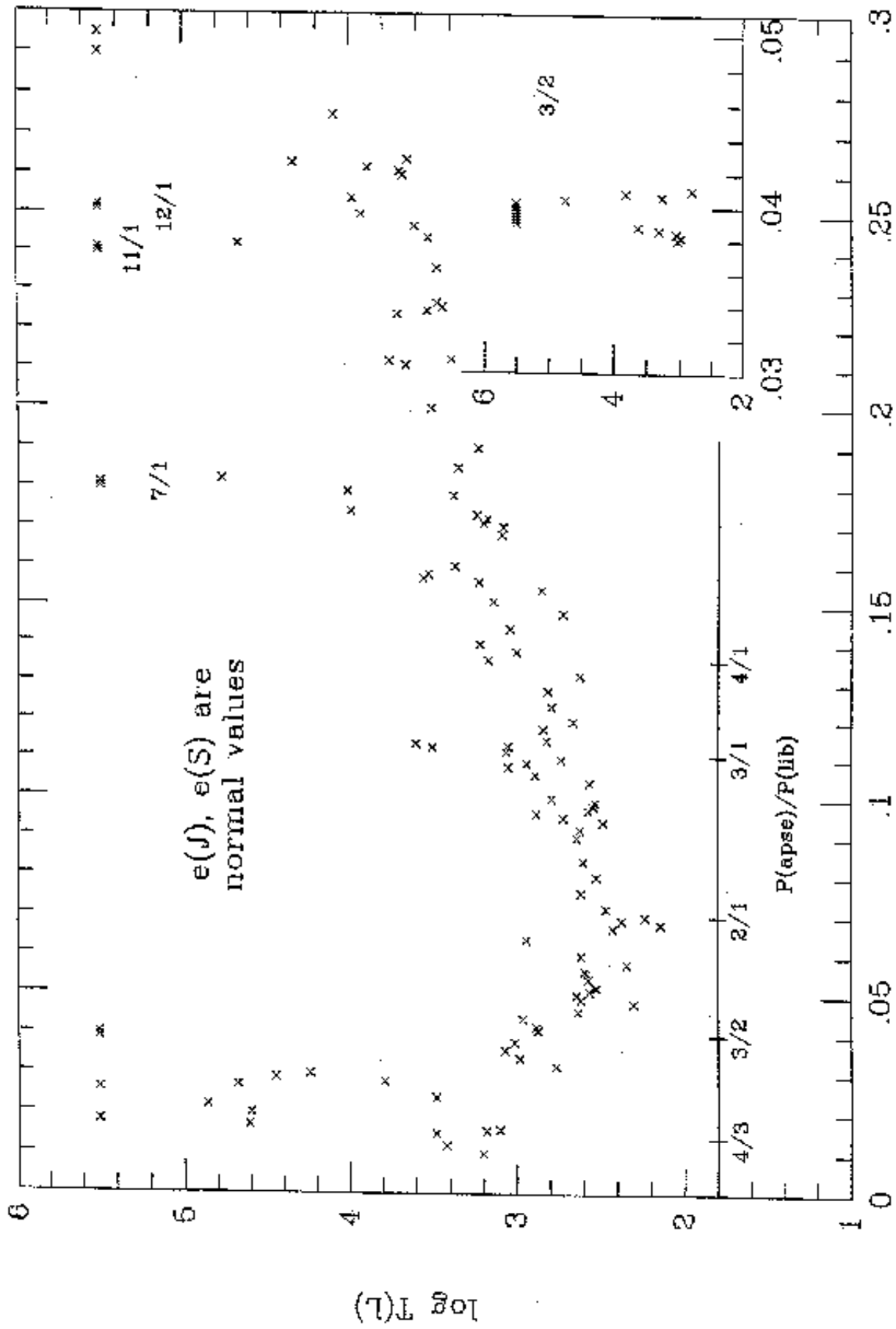


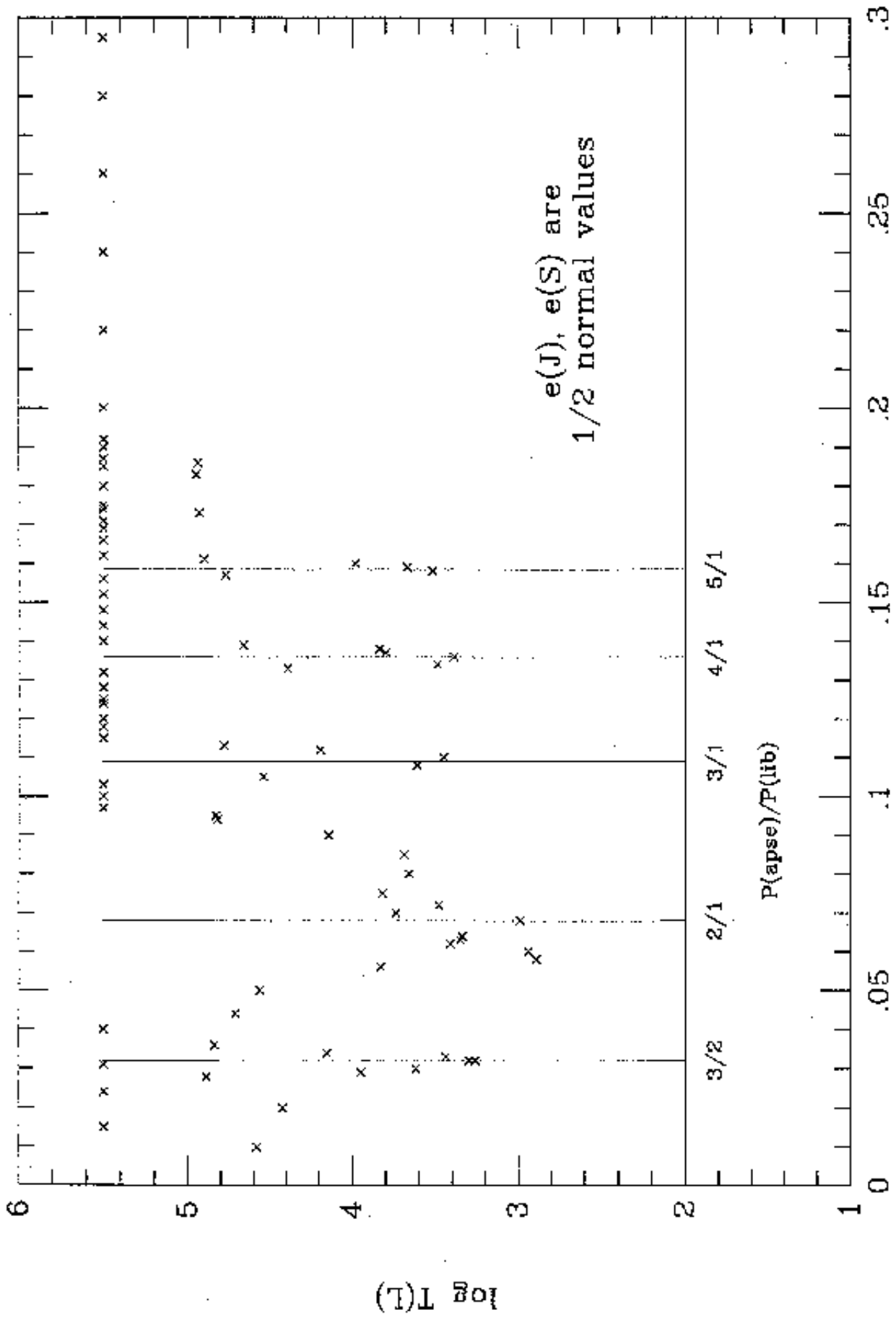
Time in Jovian orbital periods



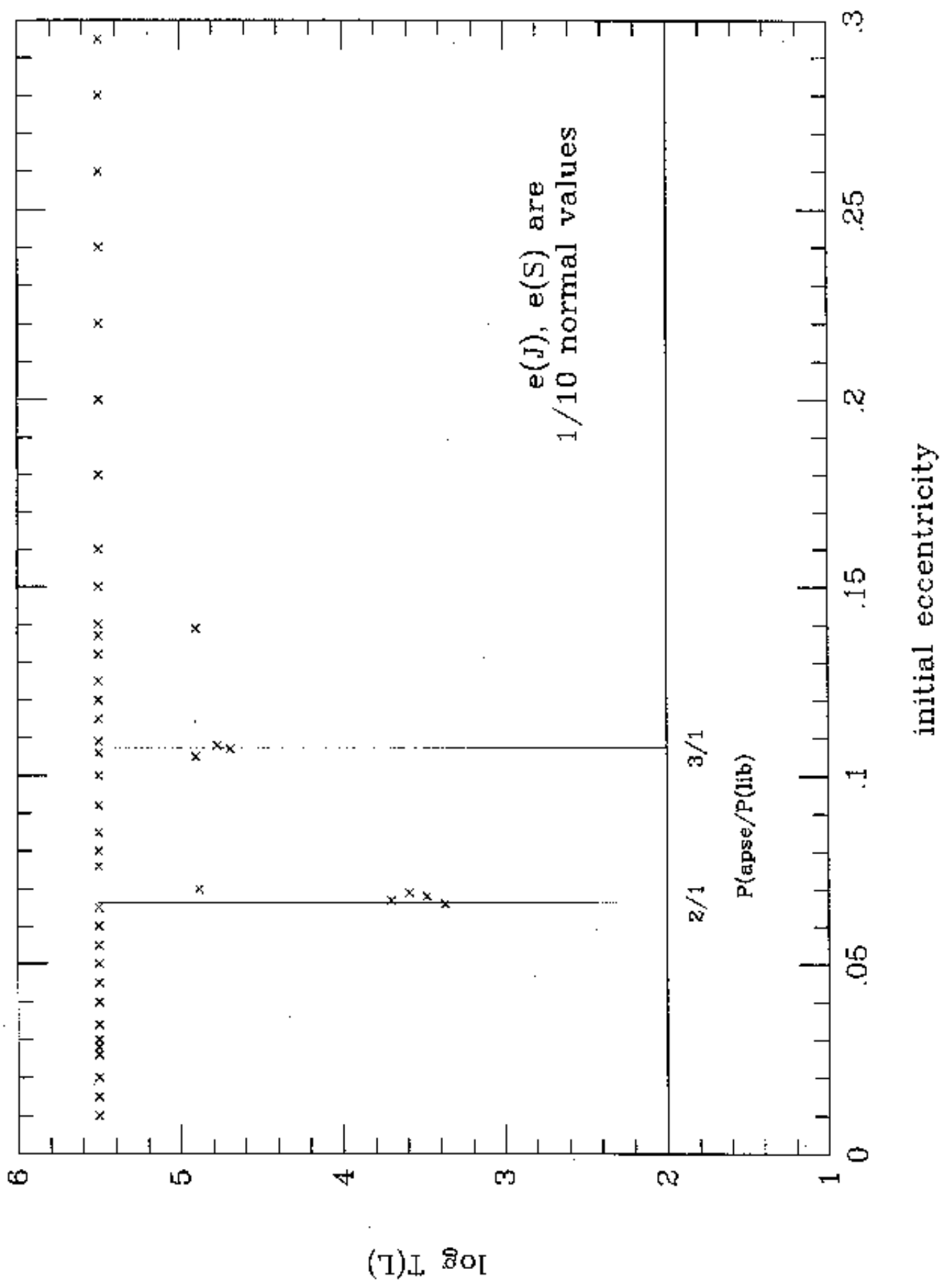
Time in Jovian orbital periods

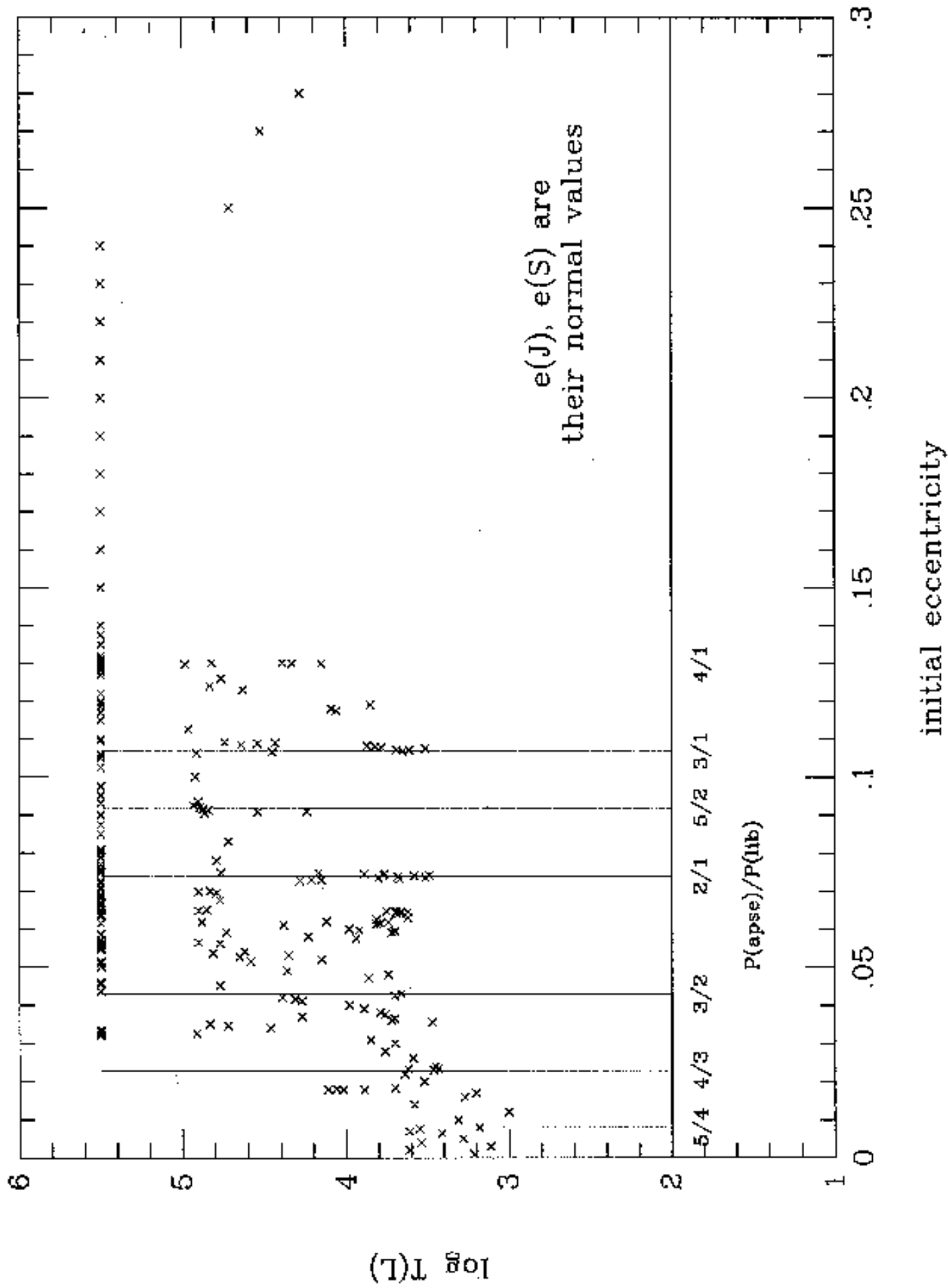






initial eccentricity





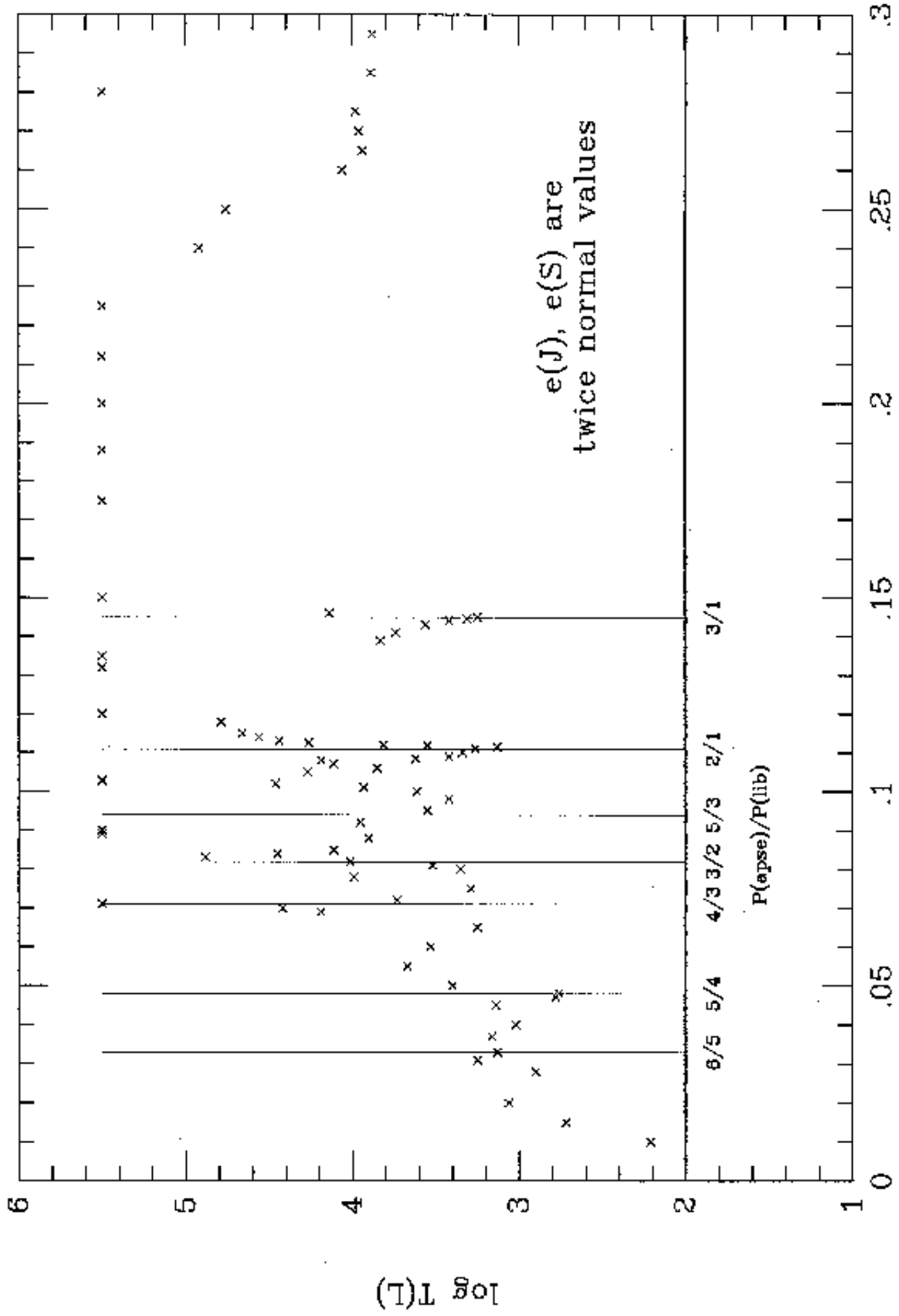
$\log T(L)$

e(J), e(S) are
their normal values

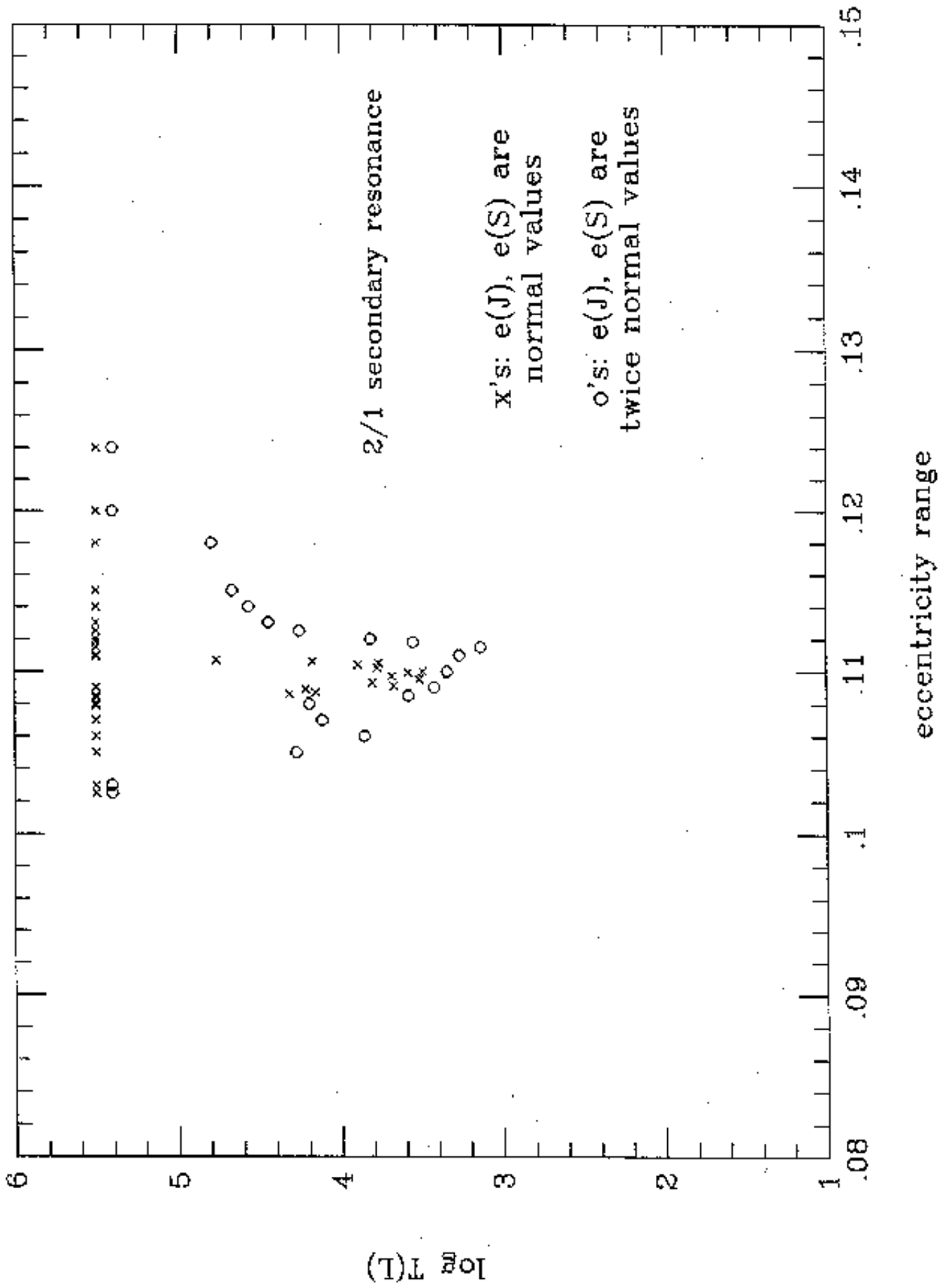
5/4 4/3 3/2 2/1 5/2 3/1 4/1

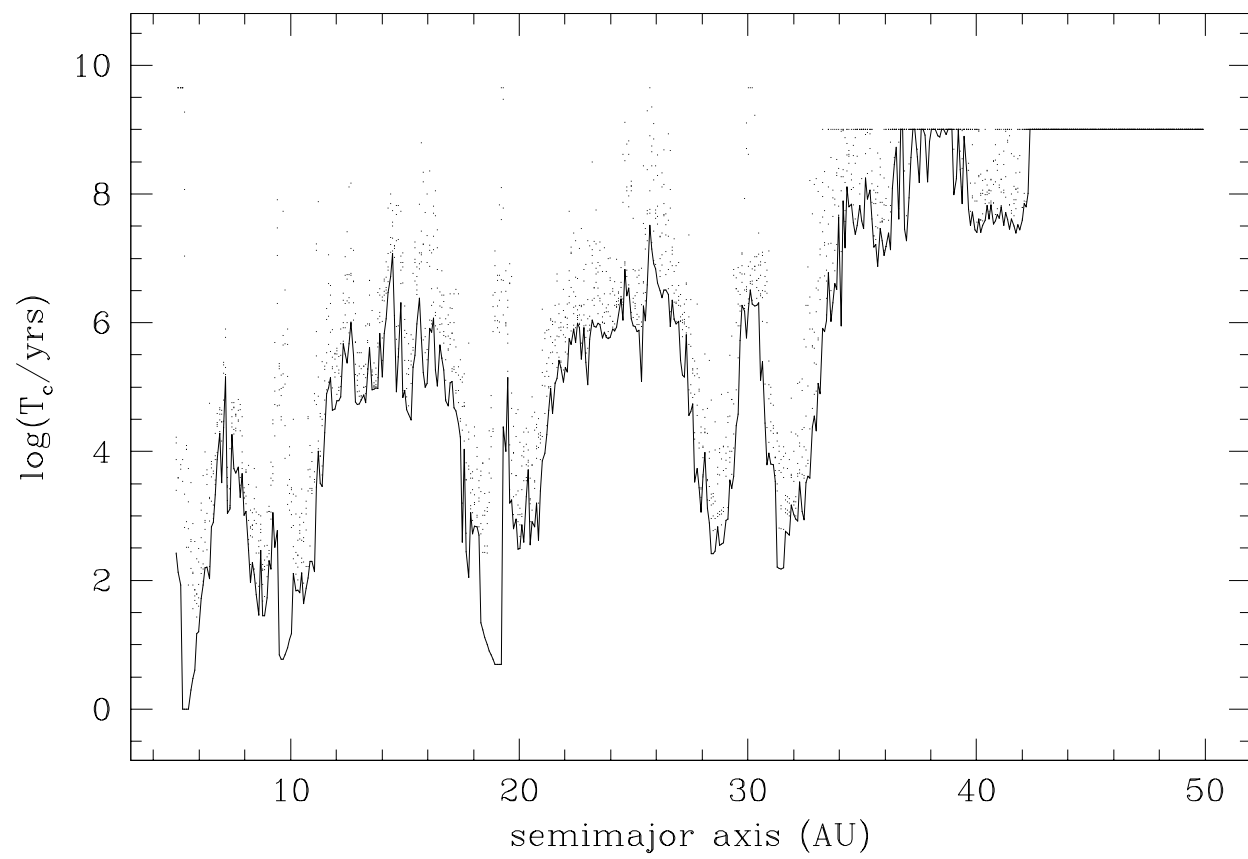
$P(\text{apse})/P(\text{ub})$

initial eccentricity



initial eccentricity





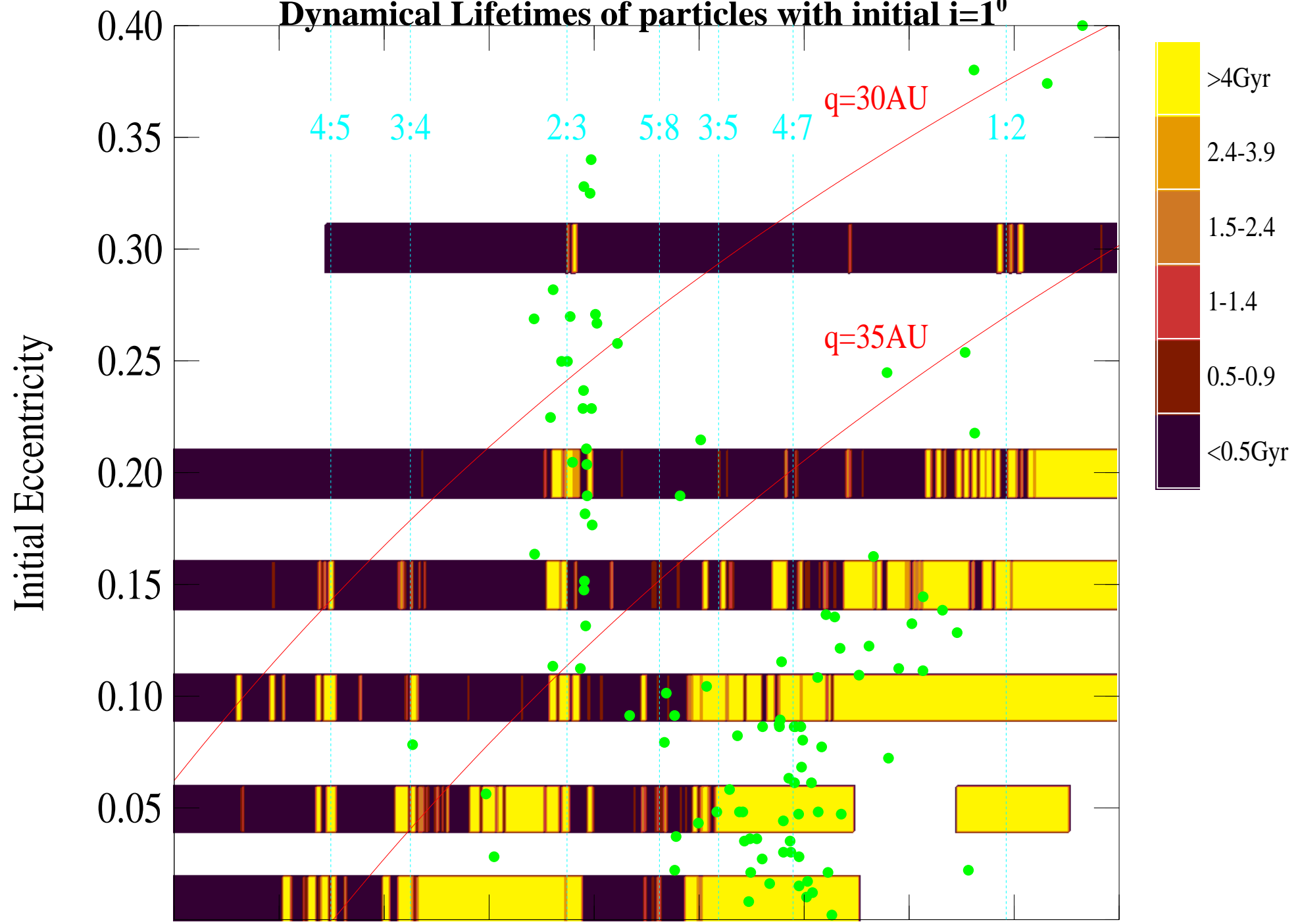
This figure "fig10.jpg" is available in "jpg" format from:

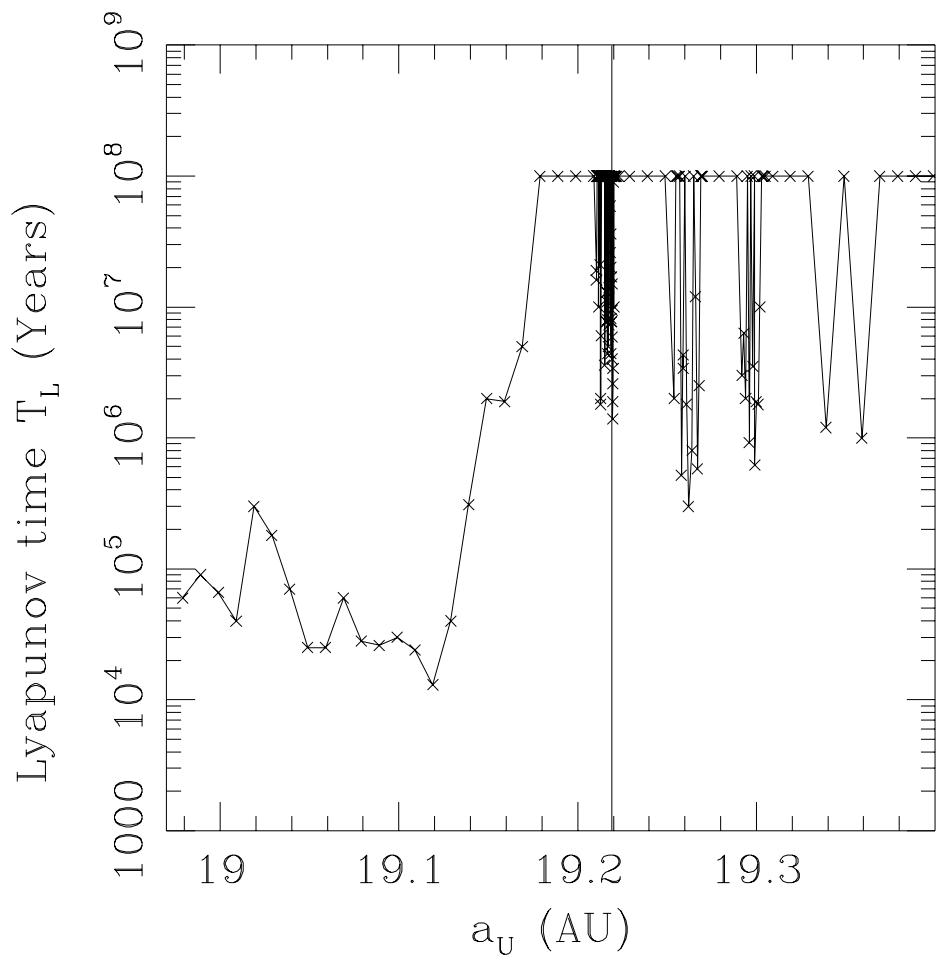
<http://arxiv.org/ps/astro-ph/0111600v1>

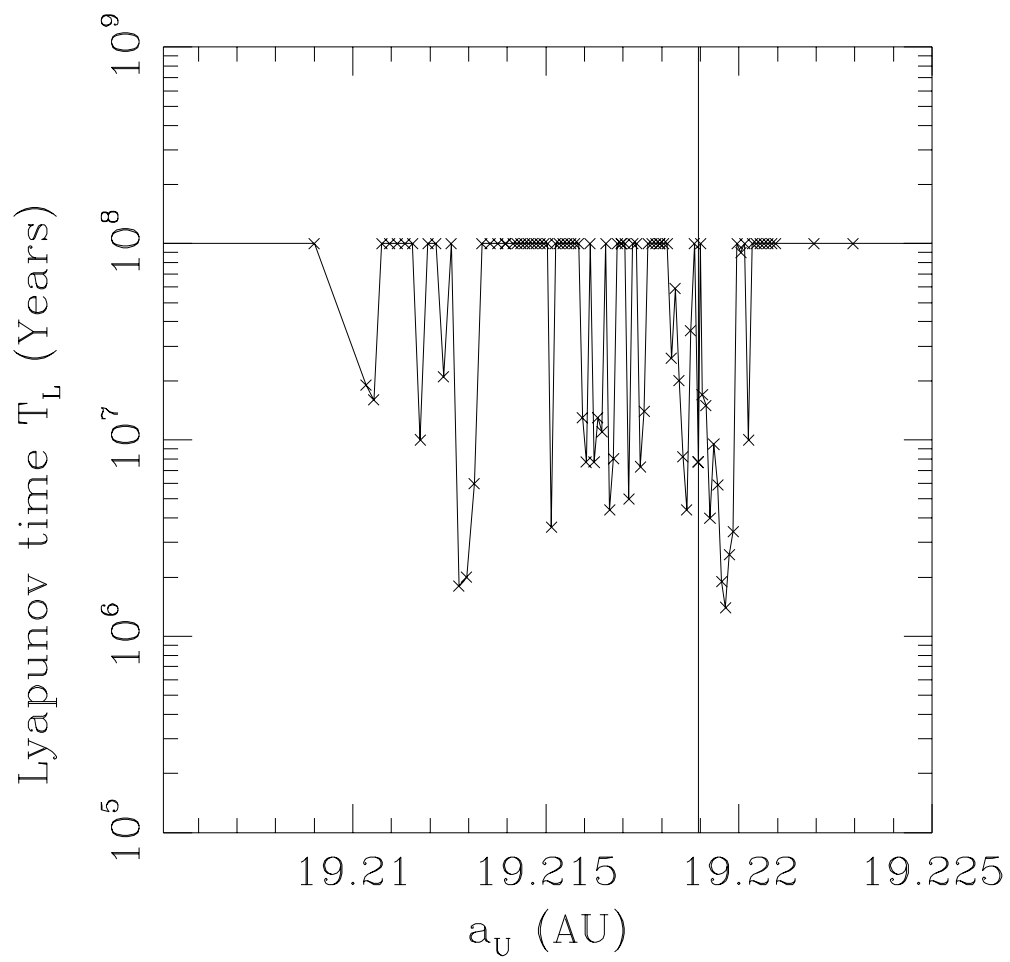
This figure "fig11.jpg" is available in "jpg" format from:

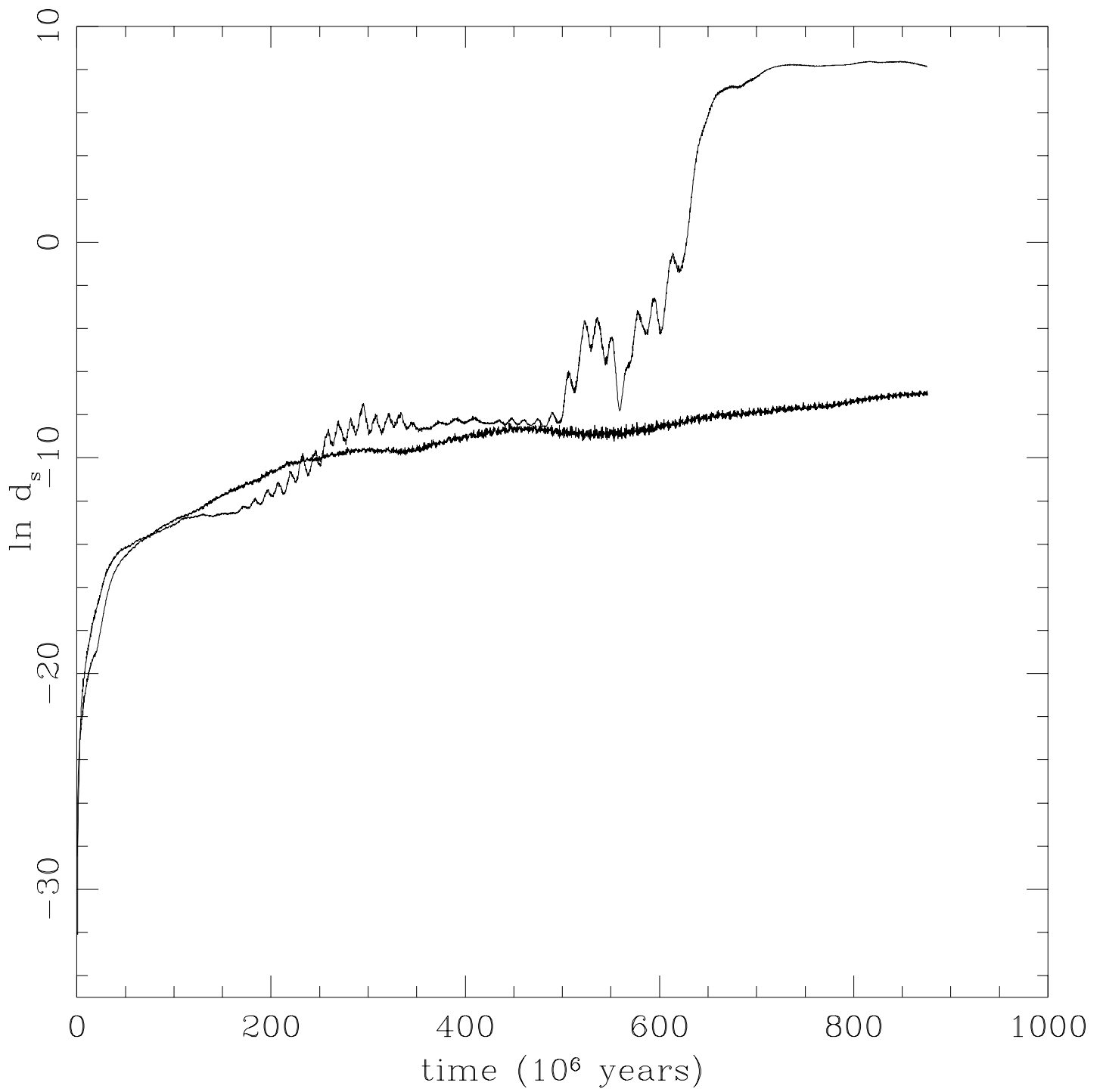
<http://arxiv.org/ps/astro-ph/0111600v1>

Dynamical Lifetimes of particles with initial $i=1^0$









FU-Runs Fig_ARAA Oct 5 17:22:04 2000

$$\sigma = 3\lambda_J - 5\lambda_S - 7\lambda_U + 3g_5 t + 6g_6 t \quad (\text{Radians})$$

